N.A.E.

R. & M. No. 2574
(10,643)
A.R.C. Technical Report

MINISTRY OF SUPPLY

AERONAUTICAL RESEARCH COUNCIL
REPORTS AND MEMORANDA

Landing of an Aircraft on a Suspended Sheet

By

J. TAYLOR, M.A.

LONDON: HER MAJESTY'S STATIONERY OFFICE
1953

TEN SHILLINGS NET

Landing of an Aircraft on a Suspended Sheet

By

J. TAYLOR, M.A.

COMMUNICATED BY THE PRINCIPAL DIRECTOR OF SCIENTIFIC RESEARCH (AIR),
MINISTRY OF SUPPLY

Reports and Memoranda No. 2574*

June, 1947

Summary.—An investigation is made into the characteristics of a freely suspended flexible sheet as a shock absorber replacing the conventional under-carriage, particular attention being given to the inertia of the sheet.

It is found that when an aircraft is dropped vertically on to the sheet the retarding force is first produced by the inertia of the sheet itself, and not until later in the descent by the reactions from the side supports of the sheet. By careful adjustments of the mass and tension of the sheet 'retardation efficiencies' exceeding 80 per cent can be achieved.

The effect of the aircraft having a forward component of velocity increases the contribution of sheet momentum. For reasonably practical landing speeds and sheet dimensions, virtually the whole of the momentum of descent is absorbed by sheet inertia. Under such conditions still higher retardation efficiencies are obtainable and, with a suitable design of aircraft keel, rebound may be entirely eliminated.

1. *Introduction*.—The successful landing of an aircraft depends on the vertical component of its velocity being reduced to zero within a limited vertical distance and without exceeding specified accelerations. For a given maximum acceleration the travel cannot be less than that which would occur if the acceleration were kept constant throughout the motion. The 'retardation efficiency' of a particular system[1] is taken as the ratio of the minimum to the actual travel.

By arranging that the vertical retarding gear is permanently on the ground it is possible to use methods which are not so restricted by weight and travel as those adopted in an ordinary undercarriage. The main limitation on ground equipment is that the travel must not be so large that parts of the aircraft at a distance from the fuselage get damaged.

This report considers the vertical retarding gear in the form of a pre-tensioned flexible sheet. Walker[1] has shown that if the sheet had negligible inertia its retardation efficiency would be low ; and although it would be increased by high initial tensioning it can never exceed 50 per cent. If the sheet has also to support the weight of the aircraft during the retarding period the retardation efficiencies are still lower, and the sheet with negligible inertia may be dismissed as impractical as an aircraft landing device.

If the suspended landing sheet is to be used it is imperative that the inertia forces must make a major contribution to the retardation. In the present investigation it is found that sheets of adequate strength have appreciable inertia and forces of the correct order are developed. It is assumed that the sheet is very flexible and has a high initial tension so that the forces in the sheet are all tensile and the tension remains constant for all deflections.

* R.A.E. Report Structures 3, received 23rd July, 1947.

The rate at which momentum is transferred to the sheet varies with the product of the tension and the mass. By the selection of a tension to give a certain force for a given static deflection it is possible to adjust the mass to give a required inertia force for a given vertical velocity.

Immediately the aircraft strikes the sheet it will start to transfer momentum to it. This will continue until the whole of the strip of sheet in contact with the aircraft is moving. The subsequent retarding force is produced by the reactions from the side supports. By a judicious combination of the tension and mass of the sheet the maximum forces in both parts of the motion can be made the same, and retardation efficiencies exceeding 80 per cent are realised.

With a vertical descent about three-quarters of the energy will have been absorbed in the first part, in which the inertia forces only are operating. When the aircraft has a forward velocity the inertia forces play an even bigger part and, at practical landing speeds and landing sheet dimensions, may absorb the whole of the vertical momentum.

2. *Use of Inertia for Retardation.*—For convenience in the mathematical treatment the landing surface is assumed to consist of a long flexible sheet suspended along two parallel edges and heavily pre-tensioned by them. Resistance to a falling body is thus due to deformation of the sheet and its own inertia.*

The sheet is assumed to be infinitely flexible so that it can exert forces only by means of tension. It is assumed further that it is infinitely elastic in stretch so that changes in tension due to any lateral deflections are negligible compared with the initial tension. The initial tension is in the transverse direction only.

Thus the sheet is represented as a series of narrow closely spaced transverse strips which act independently.

The sheet is assumed to be so heavily pre-tensioned that its own weight has a negligible effect on its distortion and that it is virtually flat when at rest.

On being struck by a moving body the sheet will behave initially as though it were infinite in width, and it is only after any waves set up in it have reached the supporting edges that the width will affect the motion. These initial forces are entirely due to the rate at which momentum is transferred to the sheet and depend on the mass of the sheet m lb/sq ft and the cross tension T lb/ft run.

Concentrating attention on the forces in a particular strip of sheet, it is assumed firstly that one point is constrained to move laterally with a constant velocity V ft/sec. Initially the whole of the strip is flat and stationary, apart from the point of contact which has a velocity V ft/sec. After a short time part of the strip each side of the moving point will have taken up the same velocity V, the remainder being still at rest. The rate at which the strip takes up its velocity will be found from the conditions of equilibrium of the strip. Assume that after a time t sec a length of strip Ut each side of the point, constrained to move with a velocity V, is moving laterally with velocity V, and the remainder at rest as shown in Fig. 1.

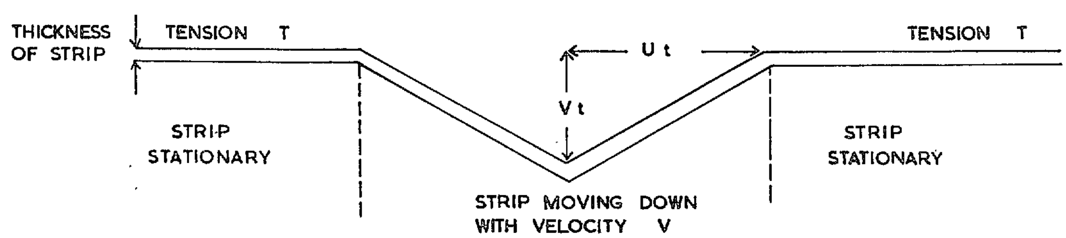

FIG. 1. Lateral displacement of the strip after time t sec. View looking along length of landing sheet.

---

* This marks the distinction between the suspended sheet under consideration and the alternative scheme for a carpet laid over elastic supports.

Taking the rate at which the strip is brought into motion (U ft/sec) to be constant, the moving strip will form a straight line at an angle ζ to the stationary part, where $\tan \zeta = V/U$.

The constrained point and adjacent strip have the same constant velocity, so that the forces at the constrained point will be in static equilibrium. Thus the force which must be applied to the sheet at the point of contact is $2T \sin \zeta$ per ft run.

The rate of change of momentum produced in the sheet by this force is $(2mU/g) \,.\, V$ per ft run due to the additional mass of $2mU/g$ per ft run per sec being given a transverse velocity V.

Equating the force to the rate of change of momentum,

$$2T \sin \zeta = 2m \frac{UV}{g},$$

$$\text{where} \quad \tan \zeta = \frac{V}{U}.$$

For small values of V compared with U, ζ will be small, and

$$U = \sqrt{\frac{Tg}{m}} . \qquad \ldots \quad \ldots \quad \ldots \quad \ldots \quad \ldots \qquad (1)$$

The transverse force at the point of contact ($2T \sin \zeta$) will be

$$2 \sqrt{\left(\frac{Tm}{g}\right)} \; V \text{ per ft run} . \qquad \ldots \quad \ldots \quad \ldots \quad \ldots \qquad (2)$$

It is shown in equation (1) that the velocity of propagation of the wave (U) is independent of the velocity of the transverse motion. Thus in the more general case of the point of contact changing its velocity with time the wave will travel at the same speed. At any instant the forces at the point of contact will be in instantaneous equilibrium, so that the transverse force will be $2T \sin \zeta$,

$$\text{where} \quad \tan \zeta = V/U,$$
$$V = \text{instantaneous transverse velocity,}$$

and for small V compared with U the transverse velocity will still be given by equation (2).

Equation (2) can now be applied to find the equations of motion of an aircraft with any shape of keel under any initial velocity conditions. In general successive approximations will be necessary and the algebra will appear rather involved so that it may be difficult to see the underlying principles. To illustrate the method the vertical descent of a weightless* aircraft on to a sheet of infinite width will be considered.

With a vertical descent the normal velocity at any point of contact will be sensibly independent of the incidence of the aircraft, and the initial retarding force on the aircraft will be given by equation (2), where V is the velocity of the c.g. As the landing sheet is of infinite width there can be no vertical forces from the sides and the retarding force will continue to be given by equation (2) throughout the descent. The velocity of the aircraft will thus continue to be reduced until the resultant force applied by the sheet balances any other forces on the aircraft and as there are no other forces the aircraft will, in fact, be brought to rest.

* For the purpose of analysis the weight and inertia are regarded as disassociated properties of a falling body. In practice gravity forces may be balanced by aerodynamic forces.

Suppose that after the aircraft has penetrated the landing sheet a distance p ft it has a velocity V ft/sec and the length of the aircraft keel in contact is c ft, then the total force on the aircraft, by equation (2) is

$$2c \sqrt{\left(\frac{Tm}{g}\right)} \cdot V ,$$

and the equation of equilibrium is

$$2c \sqrt{\left(\frac{Tm}{g}\right)} V = - \frac{W}{g} f , \quad \ldots \quad \ldots \quad \ldots \quad \ldots \quad (3)$$

where f = acceleration.

Substituting $f = V \frac{dV}{dp}$ in equation (3) we get

$$2 \frac{cg}{W} \sqrt{\left(\frac{Tm}{g}\right)} = - \frac{dV}{dp} . \quad \ldots \quad \ldots \quad \ldots \quad \ldots \quad (4)$$

If c = constant, V, and hence f, will reduce linearly with the penetration and the retardation efficiency will be 50 per cent. In no case can the contact length reduce with penetration, and to gain some idea of the effect of a varying contact length, c will be taken to vary linearly with p.

Taking $c = a + bp$ and $\frac{1}{W} \sqrt{\left(\frac{Tm}{g}\right)} = \lambda$, equation (4) reduces to

$$\frac{dV}{dp} = - 2\lambda g(a + bp) .$$

Hence

$$V = V_0 - 2\lambda g(ap + \tfrac{1}{2}bp^2) , \quad \ldots \quad \ldots \quad \ldots \quad \ldots \quad (5)$$

$$f = 2\lambda g(a + bp)\{V_0 - 2\lambda g(ap + \tfrac{1}{2}bp^2)\} . \quad \ldots \quad \ldots \quad \ldots \quad (6)$$

The maximum penetration occurs when $V = 0$,

i.e.,

$$p_m = \frac{a}{b} \left\{\sqrt{\left(1 + \frac{bV_0}{a^2\lambda g}\right)} - 1\right\} . \quad \ldots \quad \ldots \quad \ldots \quad \ldots \quad (7)$$

The corresponding maximum contact length

$$c_m = a \sqrt{\left(1 + \frac{bV_0}{a^2\lambda g}\right)} . \quad \ldots \quad \ldots \quad \ldots \quad \ldots \quad \ldots \quad (8)$$

The maximum acceleration f_m occurs when $\frac{df}{dp} = 0$,

i.e., at

$$p = \frac{a}{b} \left\{\sqrt{\left[\frac{1}{3}\left(1 + \frac{bV_0}{a^2\lambda g}\right)\right]} - 1\right\} \quad \ldots \quad \ldots \quad \ldots \quad \ldots \quad (9)$$

f_m is found by substituting the value of p, given in equation (9), in equation (6). The retardation efficiency can be found for different values of λ and is given by

$$E = \frac{V_0^2}{2 f_m x p_m} . \qquad \ldots \quad \ldots \quad \ldots \quad \ldots \quad \ldots \qquad (10)$$

The retardation efficiency is plotted in Fig. 4 for different ratios of maximum to initial contact lengths; for a given maximum penetration this ratio will vary for different rates of increase of contact length with penetration; for a given keel shape it can be changed by altering the maximum penetration. The complete acceleration-penetration curves are calculated from equation (6) and given in Fig. 5 for selected ratios of maximum to initial contact lengths. The values plotted in Figs. 4 and 5 are given in Table 1.

It can be seen that the maximum retardation efficiency is about 77 per cent and occurs for maximum contact lengths of about three times the initial contact length, but for values over $2\frac{1}{2}$ times the initial contact length the efficiency does not alter appreciably.

3. *Vertical Descent on a Landing Sheet.*—The general principles involved in the use of inertia as a means of retardation were given in section 2. With the limitation imposed on sheet width it is not possible in practice to ignore the vertical force transmitted by the sheet from the sides.

The action of a landing sheet of finite width on initial contact of the aircraft will be identical with that of an infinite sheet, and the aircraft will be retarded because of the inertia forces set up in it by the transverse wave. After the wave has reached the side supports of the sheet the effect of constraint on the sheet becomes significant, and forces corresponding to a static system are imposed. The subsequent inertia forces will then correspond to a complicated wave motion and be superimposed on the 'static force' system. For most purposes the subsequent wave motion can be ignored and the calculations will be based on this assumption.

Now the static force will depend on the width of the sheet and the initial tension. As the sheet is deflected the restoring force will depend on the tension in the sheet in its deflected position and on the angle the sheet makes with the horizontal. If the sheet were initially just taut the load per foot run would be proportional to the cube of the deflection. This would be very inefficient and an attempt must be made to have a large initial strain so that the increase in length due to the deflection is negligible and the tension is sensibly constant; the load per foot run is then proportional to the deflection. It is shown in Appendix II for a proposed rubberised fabric sheet that the increase in tension due to deflection is only a few per cent for deflections of 2 to 3 ft on a total width of 60 ft. It is assumed that the tension in the idealised sheet, considered throughout the main body of the report, is unaffected by deflections.

3.1 *Vertical Descent of a Weightless Aircraft.*—The vertical descent of a weightless aircraft on an infinite sheet has been considered in section 2. In this section the aircraft will still be taken as weightless and making a vertical descent but the effect of finite width will be considered. In section 3.2 the weight will be taken into account and in section 4 the additional effect of forward velocity will be discussed.

In the first part of the motion the finite sheet behaves in an identical manner with the infinite sheet and the acceleration penetration relationship is the same as that given in Fig. 5, Table 1, and equation (6).

$$f = 2\lambda g(a + bp)\{V_0 - 2\lambda g(ap + \tfrac{1}{2}bp^2)\} .$$

The acceleration in the second part is the same as that due to static deflection and is given by

$$f = T(a + \tfrac{1}{2}bp) \cdot \frac{p}{d}, \qquad \ldots \quad \ldots \quad \ldots \quad \ldots \quad \ldots \qquad (11)$$

where $2d$ equals the width of the sheet.

Acceleration-penetration curves are shown in Fig. 6 for sheets with the same conditions as those considered in Fig. 5, except that they have a finite width. The tension was selected by trial and error so that the acceleration at the end of the travel was the same as the maximum in the first part of the motion, the total travel being fixed by the area under the curve having to be $\frac{1}{2}V_0^2 = \frac{1}{2}f_0 \times V_0^2/f_0$. Even for the contact length of the keel constant the retardation efficiency is 81 per cent, and for a linear variation of the contact length the efficiency may become as high as 92 per cent.

3.2 *Vertical Descent of an Aircraft under Gravity.*—The acceleration-penetration relationship of a particular system is altered appreciably when an additional constant force such as gravity is imposed. The efficiency is reduced and is dependent on the ratio of the additional forces to the maximum allowable retardation.

The additional forces are gravity and aerodynamic and are grouped together as $-k$ times the initial sheet forces; thus the initial total force is $(1-k)$ times the initial sheet forces. The case $k = 0$ corresponds to the condition that the air and gravity forces balance or that the initial sheet forces are infinite. If none of the gravity forces were balanced by the air forces $k = 0 \cdot 25$ (say) would represent a total force of $-3g$ ($-4g$ from the sheet and $+1g$ due to gravity); similar results hold for other values of k.

The effect of variation of k on the acceleration-penetration relationship is considered in Appendix I for an aircraft landing with a constant length of keel. Curves are plotted in Fig. 5 and values tabulated in Table 2 for $k = 0, 0 \cdot 1, 0 \cdot 15, 0 \cdot 2, 0 \cdot 25$. It will be seen that as k increases from 0 to $0 \cdot 25$ the retardation efficiency reduces from 81 to $72 \cdot 9$ per cent.

In practice the contact length would increase with penetration and the equation of motion of the aircraft could be solved only by successive approximation even in the simple case of linear variation. As the retardation efficiency of the system with negligible gravity forces can be increased from 81 to over 90 per cent by having a moderate linear variation of contact length with penetration (Maximum contact length/initial contact length $= 2\frac{1}{2}$ to 5), it may be inferred, without doing the arithmetic, that the retardation efficiency for a $-3g$ landing with full gravity forces ($k = 0 \cdot 25$) will be increased from $72 \cdot 9$ to about 80 per cent.

3.3 *Comparison of Retardation by Means of Inertia and Static Forces.*—The vertical descent of an aircraft on a landing sheet develops inertia forces in the sheet immediately on contact, and at a later stage the forces are the same as those due to static deflections. The relative merits of both types of force as a means of retardation will now be discussed.

The retardation efficiency of a simple elastic system, under no gravity forces, is 50 per cent, and that of a pre-tensioned massless landing sheet cannot be greater. For a constant contact length and with the sheet initially just taut the retardation efficiency is 25 per cent; pre-tensioning improves the efficiency until it reaches 50 per cent for the case of a sheet with a very high initial strain. If the contact length increases with penetration, as would happen with an ordinary aircraft, the efficiency is reduced.

The retardation efficiency of an inertia system, under no gravity forces, is 50 per cent for a constant contact length but is in excess of 75 per cent for a contact length increasing linearly to between $2\frac{1}{2}$ and 5 times its initial contact length (Fig. 4).

A particular condition of combined inertia and static forces is taken from Fig. 6, and the effects of inertia and static forces taken separately are shown in Fig. 8. The inertia forces have an efficiency of 77 per cent and the static forces an efficiency of 41 per cent.

The above efficiencies are independent of the magnitude of the accelerations. When gravity forces are superimposed the ratio of these to the maximum acceleration is important, and for normal maximum permissible landing accelerations the efficiencies are appreciably reduced, particularly when the efficiency with gravity absent is less than 50 per cent. With a maximum permissible retardation of $3g$ the just taut massless sheet would have a zero efficiency[1] even with a constant contact length, *i.e.*, it would just take an infinite distance to retard the aircraft if $3g$ is not to be exceeded.

These difficulties arise because, in the early part of the retardation, the static forces are less than the gravity forces and the aircraft is actually increasing its velocity.

The forces developed by virtue of the inertia of the sheet do not suffer this disadvantage, for they are proportional to the velocity of the aircraft, and may exceed the gravity forces immediately contact is made.

As the aircraft penetrates further into the sheet the velocity decreases and the inertia forces become less and less, until eventually they just balance the gravity forces whilst the aircraft is still moving. The elastic forces, depending on deflections, would increase as the aircraft penetrated further. Thus the combination of elastic and inertia forces shown in Fig. 6 makes use of the best of both systems ; the inertia forces are the more important and absorb at least three quarters of the energy for all ordinary increases in contact length with penetration.

An important difference between 'inertia' and 'static' retardation arises when a sheet is designed for landings with full gravity forces and is then used with gravity forces absent. The maximum retardation due to static forces for a given impact velocity is reduced as the unbalanced gravity forces are reduced. In the inertia system the maximum retardation occurs immediately on contact and is increased as the unbalanced gravity forces are reduced.

A further difference arises in connection with rebound after landing. The energy absorbed by an elastic system is mainly recoverable, whereas that due to the inertia of the sheet is not recoverable by the aircraft.

4. *Landing with Forward Velocity on to a Sheet.*—If the aircraft has a forward velocity on landing the conditions of the landing sheet are rather different. With sufficiently high forward velocities the sheet of finite width would behave in the same way as the infinite one ; the condition for this is satisfied if the wave in a particular strip of sheet, which commences as the bow of the aircraft goes over it, has not reached the side support by the time the stern of the aircraft has passed it.

A good indication of the behaviour of the aircraft on landing with a reasonable forward velocity can be obtained from an examination of its behaviour on the infinite sheet.

Consider an aircraft with a keel of general shape striking the sheet. The force due to an individual strip is proportional to the transverse velocity given to it. The velocity will be the component of the total velocity in the direction normal to the keel surface at that point, the tangential component having no effect except in so far as there is friction between the two surfaces. There will be some point near the tail at which the velocity is along the tangent to the keel ; forward of this point the normal component of the velocity will be into the sheet, and aft of this point it will be away from the sheet. Thus at any point aft of the transition point there will be no force between the sheet and the aircraft.

As the aircraft penetrates further into the sheet the force on the nose portion increases and its centre of pressure acts further forward. At the same time the downward component of the aircraft velocity reduces and the transition point moves forward. These effects both tend to increase the nose-up pitching moment on the aircraft. The pitching moment tends to give the aircraft an angular velocity, which in turn develops a restoring moment from the sheet so that eventually the aircraft would tend to have a limiting angular velocity.

It is hardly possible in conventional aircraft to prevent this high nose-up pitching moment developing, but it is possible to keep the angular displacement small by having a forward position of the aircraft c.g. relative to the centre of the keel so that on initial contact there is a nose-down pitching moment.

The main trouble with a high angular nose-up velocity is that the incidence of the aircraft increases with penetration and the total acceleration is roughly proportional to the incidence, so that the aircraft may receive more vertical energy than it gave up and rebound with a higher vertical velocity.

If the angular velocity were zero the incidence would reduce steadily, due to the loss of the vertical component of the velocity, and the vertical velocity of rebound would be smaller than the impact value. In the particular case of a flat keel, horizontal and with a constant contact length, the retardation would reduce to zero at maximum penetration and there would be no rebound.

5. *Numerical Examples.*—The salient features of the use of inertia to retard an aircraft have been illustrated in the preceding paragraphs by means of the simple case of a vertical drop of an aircraft on a sheet with a contact length increasing linearly with penetration. The problem of landing with a high forward velocity has only been discussed in general terms, as a solution can only be found by successive approximation.

The general case of an aircraft landing with a linear and an angular velocity is considered in Appendices II and III for a keel with a longitudinal shape consisting of a central portion of length $2e$ and nose and tail portion with radii R_L and R_T. The equations of motion are formed in Appendix II and the numerical method of solution illustrated in Appendix III with values of R_L, R_T and b representative of a *Hotspur*.

The equations of motion are quite general but they will usually be applied to cases where one of the horizontal and vertical components is small compared with the other; for landings on aerodromes the horizontal velocity would be very much the larger, and on carriers the aircraft may be caught by an arrester wire so that the horizontal velocity was small by the time the aircraft struck the sheet. In the case of a vertical drop the acceleration-penetration curve can be calculated directly for the linearly tapered keel, but in the case of the landing with high horizontal velocity successive approximation is necessary in both cases and the numerical work involved is high.

5.1 *Numerical Example of a Vertical Descent.*—Calculations have been made on the lines given in Appendices II and III to show the effect of the mass of the sheet on the landing of a *Hotspur* at 7000 lb on to a sheet with a cross tension of 3600 lb/ft.

For convenience in the calculations exact values have been chosen for the parameter $\lambda \left(= \frac{1}{W} \sqrt{\left(\frac{Tm}{g}\right)}\right)$ rather than for the mass m lb/sq ft of the sheet. Typical acceleration-penetration curves are shown in Fig. 9. It will be seen that the retardation efficiency can be made high by having a very heavy sheet, but that the tension is rather low and the maximum penetration is correspondingly high.

The variation of maximum accelerations and penetrations with impact velocity is given in Fig. 10. It can be seen that the maximum penetration is about $2 \cdot 5$ ft even with zero impact velocity, but that it does not increase appreciably for velocities up to 10 ft/sec in the case of the heaviest sheet. At velocities as high as 20 ft/sec the maximum penetrations and accelerations depend greatly on the mass of the sheet. With the massless sheet they are $4 \cdot 52$ ft and $5 \cdot 33g$ respectively, but for the heaviest sheet they are $3 \cdot 27$ ft and $2 \cdot 54g$.

5.2 *Numerical Example of a Landing with Forward Velocity*.—The aircraft landing with a high forward velocity obtains its retardation more by the inertia forces set up in the sheet than by the forces due to the static deflection, and the effect of width of sheet is not great (section 4).

The retardation-penetration relationship has been found for the *Hotspur* landing at a weight of 7000 lb with various impact velocities onto an infinite sheet with a cross-tension of 3600 lb/ft and various masses of sheet. The effect of the finite width of sheet will only influence the motion near the end of the travel and will be fairly small.

Fig. 11 gives the retardation-penetration curve for a particular landing velocity and two positions of the aircraft c.g. When the c.g. is near the centre of the keel there is a great tendency for the nose of the aircraft to be forced up so that the vertical force continues to increase even after the sheet has had its maximum deflection and is returning to the initial position. The rebound velocity thus received by the aircraft is of about the same magnitude as the impact velocity. When the c.g. is well forward of the centre of the keel, the energy taken up by the aircraft is considerably less and the rebound velocity correspondingly smaller.

6. *Design Characteristics*.—The design of the sheet will depend on the size and weight of the aircraft and conditions of landing. The properties of the sheet are fixed if a particular aircraft is to experience an optimum retardation efficiency with a certain maximum acceleration and penetration for a given vertical component of landing velocity. No attempt is made in the present report to assess the loss of retardation efficiency of a particular landing sheet by using it for aircraft with ratios of weight to length different from the ratio which gives optimum efficiency.

The forward velocity of the aircraft has a considerable influence, as it varies the mass of sheet brought into motion in a given time. Landing with high or negligible forward velocities are the two cases normally met in practice. The retardation with high forward speeds is dependent only on the inertia forces set up in the sheet, and a given inertia force can be achieved by altering the tension in a sheet of any mass. With negligible forward velocities the first part of the motion is controlled by inertia forces and the second by static forces. For the most efficient system the maximum inertia and static forces will be the same.

6.1 *Properties of the Landing Sheet*.—General properties of the sheet can be found by considering the aircraft with a contact length which remains constant throughout the motion. This average contact length will probably be about half the overall length of the aircraft. The lengths of a large number of aircraft are compared with their weight in Fig. 12 and Table 3. There is considerable scatter, but the weight in lb is seldom much greater than 10 times the square of the length in ft. The characteristics of the sheet to cope with aircraft with such a weight to length ratio will be determined.

Assuming the contact length c equals half the length of the aircraft,

$$\frac{W}{c} = 40c = 20 \times (\text{length of aircraft}). \qquad \ldots \quad \ldots \quad \ldots \quad (12)$$

It can be shown from equation (6) that for a given mass and tension of sheet the accelerations given to the aircraft by the sheet are proportional to $V_0/(W/c)$, which by equation (12) is proportional to V_0/c. Thus for airborne landings the retardation would be proportional to V_0/c and the maximum penetration consequently proportional to V_0c. For a given impact velocity the maximum penetration would be proportional to c. For similarly shaped aircraft the maximum allowable penetration is evidently proportional to the length, and it seems worth while to take advantage of this in allowing lower retardations.

With landings such as those experienced on a carrier, at low forward velocity on impact the aircraft would not be airborne and the total acceleration is reduced by the constant gravity plus air force, and the penetration would not be proportional to V_0c. It may be possible to use the same sheet for aircraft of different weight without much change in efficiency if the tension can be adjusted to maintain the required maximum penetrations.

It is probable on carriers that the design of deck may prohibit larger penetrations for larger aircraft. When this is so the sheet would have to be adjusted to give the same maximum acceleration for all sizes of aircraft. It should be possible to cope with a moderate range of weight to length ratios by adjusting the tension in the sheet.

Appendix I compares the retardation with penetration for different ratios (k) of the gravity and air forces to the initial sheet forces. Table 2 gives the relationship together with retardation efficiency and the mass and tension of the sheet. For any value of k the efficiency is decided by the mass of the sheet, and the maximum acceleration is then given by the tension.

It can be seen in Table 2 that the mass of the sheet to give best efficiency is $0 \cdot 309\ W/cd_0$ when the gravity plus air forces are negligible, rising to $0 \cdot 454\ W/cd_0$ when the gravity plus air forces are a quarter of the sheet forces (this would occur when the maximum acceleration was $-3g$, made up of $-4g$ sheet forces and $+1g$ gravity plus air forces). The corresponding tensions are $0 \cdot 808 \dfrac{Wd_0}{c}\, g \dfrac{n_0'^2}{V_0^2}$ for $k = 0$, rising to $0 \cdot 979 \dfrac{Wd_0}{c}\, g \dfrac{n_0'^2}{V_0^2}$ for $k = \frac{1}{4}$.

Take as a specific example the problem of retarding an aircraft at vertical velocities up to 20 ft/sec within about 2 ft. With 100 per cent efficiency an acceleration of $-3 \cdot 1g$ would be developed. Now the actual efficiency will be about 75 per cent, so that the acceleration will be about $-4g$. Assuming the air forces to be negligible the gravity plus air forces will be $+1g$, and with $k = 0 \cdot 2$ the sheet forces are $-5g$ and the total force $-4g$. For $k = 0 \cdot 2$ the efficiency is $75 \cdot 5$ per cent, so that the maximum penetration is $2 \cdot 05$ ft. To keep within 2 ft and $4g$ the velocity would have to be restricted to $19 \cdot 75$ ft/sec.

The following sheet properties can be found from Table 2.

$$\text{Weight of sheet} = 0 \cdot 414 \frac{W}{cd_0} \text{ lb/sq ft.} \qquad (13)$$

$$\text{Cross tension} = 0 \cdot 943 \frac{Wd_0}{c} \frac{n_0'^2}{V_0^2} g \text{ lb/ft run.} \qquad (14)$$

$$\text{Stress} = 0 \cdot 987 \frac{n_0'^2}{V_0^2} g d_0^2 \rho \text{ lb/sq in.} \qquad (15)$$

Substituting $n_0' = 4$, $V = 20$, in equations (14) and (15),

$$\text{Cross tension} = 1 \cdot 215 \frac{Wd_0}{c} \text{ lb/ft run.} \qquad (16)$$

$$\text{Stress} = 1 \cdot 270\ \rho d_0^2 \text{ lb/sq in.} \qquad (17)$$

With a sheet width ($2d_0$) of 60 ft the stress would be

$$1140\rho \text{ lb/sq in}$$

If it is thought that the tensile stress is too high, it is possible to get similar results at only slightly reduced efficiencies by increasing the weight of the sheet and keeping the tension per foot the same, but if an attempt is made to reduce the weight of the sheet without at the same time reducing the tension, and consequently the maximum retardation, the efficiency will fall off rapidly.

The actual sheet forces are higher than those given by assuming the sheet to be a series of closely spaced transverse strips. The effect will be greater for the part of the motion in which the predominant forces are static forces so that the maximum static forces will be greater. As the static forces increase rapidly with penetration this may mean a considerable reduction in efficiency.

It is advisable, therefore, in designing a sheet for a particular type of aircraft, to avoid high static forces even at the expense of a slight loss of efficiency by making the mass of the sheet slightly higher, and the tension correspondingly lower, than that given by calculation.

6.2 *Properties of the Aircraft.*—The aircraft undergoes two types of loading during an ordinary landing, one due to the inertia forces and the other due to the static forces. With a well-designed sheet the initial tensile strain will be high, so that the tension will be sensibly constant throughout the motion and the pressure imposed on the fuselage will be equal to the tension times the curvature.

By knowing the total load per foot run of the keel at any position the extent to which the sheet must wrap itself round the fuselage can be calculated. When the retardation is achieved by inertia loads the load per foot run will be proportional to the component of the velocity of the aircraft normal to the direction of the keel at the position considered. When static forces are operative the load per foot run will be proportional to the depth of penetration.

With a vertical drop the maximum load per foot run of keel will be greater near the centre of the keel for either type of loading; with inertia loading this is because the velocity will have reduced by the time the sheet has made contact with the forward and aft portions, with static forces it is because the deflections are smaller.

Landing with high forward velocities offers a different problem. The retardation is almost entirely due to inertia forces, and near the bow the forward velocity will contribute considerably to the normal velocity and high loads will be experienced. Physically this can be seen to be due to the aircraft trying to 'plough' its way into the sheet.

7. *Conclusions.*—Replacing the undercarriage of an ordinary aircraft by a landing deck on the ground opens out new possibilities regarding methods of retarding an aircraft on landing.

In particular the inertia of the landing deck can be utilised. The retarding forces over a given contact length will be dependent on the normal velocity. The advantage over most elastic systems is that large forces can be developed before appreciable deflections are attained.

For landings with high forward velocities the retardation is almost entirely inertial and the forces are proportional to the product of the mass and the tension of the sheet; any mass can be used provided the corresponding tension is not too great for the material of the sheet.

Landings with negligible forward velocities make use of inertia forces in the first part and static forces in the second part of the landing. By increasing the mass of the sheet the inertia forces are increased and the maximum static forces reduced, and at some mass, for a given type of landing, the maximum inertia and static forces are the same. The mass of the sheet would have to be $0 \cdot 309\ W/cd_0$ lb/sq ft if the gravity plus air forces were negligible compared with the sheet forces rising to $0 \cdot 414\ W/cd_0$ lb/sq ft when the gravity air forces plus were a quarter of the sheet forces,

where W lb = weight of aircraft,

c ft = average contact length

$2d_0$ ft = sheet width.

The tension in the sheet can then be adjusted to give the required maximum acceleration.

Retardation efficiencies of more than 90 per cent can be achieved when the gravity plus air forces are negligible compared with the sheet forces ; even with gravity and air forces one-quarter of the sheet forces, efficiencies of more than 80 per cent should be achieved.

In order to achieve these high efficiencies it is advisable to give the deck a high initial strain. With rubberised fabric and reasonable deck widths this is automatically achieved with the high tensions required, but with metals (*e.g.*, steel net) a spring would be required to attach the sheet to the side supports.

REFERENCE

No.	*Author*	*Title, etc.*
1	P. B. Walker	Retardation Efficiency of Shock-absorber and Arrester Gear. *Jour. Roy. Aero. Soc.* October 1945.

T		Cross tension of sheet, lb/ft
m		Weight of sheet, lb/sq ft
ρ		Specific gravity of the sheet material
$2d$		Width of sheet, ft
h		Thickness of sheet, ft
W		Weight of aircraft, lb
I		Pitching moment of inertia of aircraft, lb in.^{2}
λ	$=$	$\frac{1}{W}\sqrt{\left(\frac{Tm}{g}\right)}$
U		Velocity of a transverse wave set up in a strip of the sheet, ft/sec
ζ		Angle taken up by the moving strip relative to undeflected position
V		Velocity of aircraft, ft/sec
ψ		Angle the velocity makes with horizontal
f		Vertical acceleration of aircraft, ft/sec
p		Penetration into sheet, ft
c		Length of aircraft keel in contact with the sheet, ft
$(a + bp)$		Contact length when varying linearly, ft

When keel is made up of a straight central portion with radii at nose and tail,

$2e$		Length of central portion of keel
R_L		Radius of curvature at nose
R_T		Radius of curvature at tail
t		Time, sec
V_0, f_0		Initial values of V and f
f_0	$=$	$-n_0'g = -n_0(1-k)g$
$-n_0 g$		Initial acceleration due to sheet
k		Ratio of air plus gravity forces to sheet forces
$f_m\, p_m\, c_m$		Maximum values of f, p, c
E		Retardation efficiency, $= \dfrac{V_0^2}{2f_m \cdot p_m}$

For keel shape made up of a straight portion length $2e$ and nose and tail of radii R_1 and R_T.

x_1	Moving axis in direction of velocity V
x_2	Moving axis perpendicular to V and upwards
x_3	Moving axis forming right-handed system of axes with x_1 and x_2
Ω	Rotation of moving axes
$-D$	Sheet force in direction $x_1 = -$Drag
L	Sheet force in direction $x_2 =$ Lift
D_A, L_A, M_A	Air forces corresponding to D, L, M
M_V	Moment due to linear velocity V
M_ω	Moment due to angular velocity ω

d	$=$	$D/\lambda VW$
l	$=$	$L/\lambda VW$
m_V	$=$	$M_V/\lambda VW$
m_ω	$=$	$M_\omega/\lambda\omega W$
d_A	$=$	D_A/W
l_A	$=$	L_A/W
m_A	$=$	M_A/W
α		Angle keel makes with x_1
θ_L		Angle tangent at point of entry of nose makes with x_1
θ_T		Angle tangent at point of exit of tail makes with x_1
θ		Angle the tangent at current point makes with x_1
α_1	$=$	$\alpha + \psi$ = angle stronger portion of keel makes with horizontal
θ_{L1}	$=$	$\theta_L + \psi$
θ_{T1}	$=$	$\theta_T + \psi$
R		Radius of curvature at θ
$\bar{x}, \bar{y}$		Co-ordinates of c.g. relative to centre of keel, along and at right-angles to keel direction
V_x, V_y		Component of V in directions x and y
θ	$=$	ϕ is point at which normal velocity is zero.

APPENDIX I

Aircraft Dropping Vertically under Gravity

Suppose the aircraft has a constant length of keel a and drops with an initial acceleration $-n_0'g = -n_0(1 - k)g$,

where $-n_0 g$ = the initial acceleration due to the sheet forces,

$kn_0 g$ = the acceleration due to the algebraic sum of gravity and aerodynamic forces.

Usually the aerodynamic forces will be negligible and $n_0 k = 1$, but the algebra is not made more complicated by keeping the general form of the acceleration.

Let p, V, f be the displacement, velocity and acceleration respectively after time t, and 0, V_0, f_0, the initial values.

After time t,

$$\text{acceleration due to sheet inertia forces} = -\ 2\lambda a V,$$

$$= -\ 2\lambda a V_0 \cdot \frac{V}{V_0} = -n_0 g \cdot \frac{V}{V_0} .$$

Hence $$f = -n_0 g \left(\frac{V}{V_0} - k\right) = + f_0 \cdot \frac{V - V_0 k}{V_0(1 - k)} . \qquad \ldots \quad \ldots \quad \ldots \quad (18)$$

Substituting $f = V\dfrac{dV}{dp}$ in equation (18), we get

$$V\frac{dV}{dp} = -n_0 g \left(\frac{V}{V_0} - k\right) .$$

Hence $$\frac{n_0 g}{V_0} p = -\int_{V_0}^{V} \frac{V\,dV}{V - kV_0} .$$

After integrating, this equation can be reduced to

$$\frac{n_0 g}{V_0^2}(1 - k)p = (1 - k)^2 \left[1 - \frac{V - kV_0}{V_0(1 - k)} - \frac{k}{1 - k}\log\frac{V - kV_0}{V_0(1 - k)}\right] .$$

Hence $$\frac{-f_0}{V_0^2} p = (1 - k)^2 \left[1 - \frac{f}{f_0} - \frac{k}{1 - k}\log\frac{f}{f_0}\right] . \qquad \ldots \quad \ldots \quad \ldots \quad (19)$$

If the sheet were infinite a steady state would be reached when $V = V_0 k$. In the particular case of the aircraft airborne ($k = 0$) the aircraft would be just brought to rest (*see* equation (7)).

The sheet of finite width behaves the same as the infinite one in the first part of the motion, but after a certain time the restoring force is very nearly that given by the static deflection,

i.e., $$f = -\frac{2T}{W} \cdot a\frac{p}{d}g + n_0 kg ,$$

therefore $$\frac{f}{f_0} = \frac{\dfrac{2T}{W}\dfrac{p}{g}a}{n_0(1-k)} - \frac{k}{1-k},$$

$$= \frac{-f_0 p}{V_0^2}\left\{\frac{V_0^2}{n_0^2(1-k)^2}\cdot\frac{2T}{Wg}\cdot\frac{a}{d}\right\} - \frac{k}{1-k}. \qquad \text{.. .. ..} \qquad (20)$$

The acceleration-penetration curve consists of two parts, the first part being given by equation (19) and the second part by equation (20). For a given value of k the shape of the curve with non-dimensional co-ordinates $(-f_0/V_0^2)p$, f/f_0 is fixed. To give optimum retardation efficiency the slope of the straight line, given by equation (20), must be adjusted so that $f/f_0 = 1$ at the maximum penetration as well as on initial contact, the area under the curve f/f_0, $(-f_0/V_0^2)p$ being $\frac{1}{2}$.

The straight line passes through the point $(-f_0/V_0^2)p = 0$, $f/f_0 = -k/(1-k)$; the point $(-f_0/V_0^2)p = (-f_0/V_0^2)p_m$, $(f/f_0 = 1)$ can be found by trial and error of values of p_m until the area under the curve is $\frac{1}{2}$.

Substituting $\dfrac{-f_0}{V_0^2}p = \dfrac{-f_0}{V_0^2}p_m$, $\dfrac{f}{f_0} = 1$ in equation (20) we get

$$1 = \frac{-f_0}{V_0^2}p_m\left\{\frac{V_0^2}{n_0^2(1-k)^2}\frac{2T}{Wg}\cdot\frac{a}{d}\right\} - \frac{k}{1-k}.$$

Hence $$\frac{-f_0 p_m}{V_0^2} = \frac{1}{1-k}\Big/\left\{\frac{V_0^2}{n_0^2(1-k)^2}\cdot\frac{2T}{Wg}\cdot\frac{a}{d}\right\}.$$

Now the initial sheet force $= -2\lambda a g V_0 = -n_0 g$.

Therefore $$\frac{V_0}{n_0} = \frac{1}{2\lambda a} = \frac{W}{2a}\sqrt{\left(\frac{g}{Tm}\right)}. \qquad \text{.. .. ..} \qquad (21)$$

Hence $$\frac{-f_0}{V_0^2}p_m = \frac{1}{1-k}\Big/\left\{\frac{W^2}{4a^2(1-k)^2}\cdot\frac{g}{Tm}\cdot\frac{2T}{Wg}\cdot\frac{a}{d}\right\},$$

$$= \frac{1}{1-k}\Big/\frac{W}{2ad(1-k)^2}\cdot\frac{1}{m} = m\,(1-k)\cdot\frac{2ad}{W}.$$

Thus for a given value of k a maximum retardation efficiency can be achieved by selecting the mass of the sheet to be given by

$$m = \frac{-f_0}{V_0^2}p_m\cdot\frac{1}{1-k}\cdot\frac{W}{2ad}, \qquad \text{.. .. ..} \qquad (22)$$

and is independent of the tension.

The value of the tension can be chosen to give the required maximum retardation.

Combining equations (21) and (22) we get

$$T = \frac{1}{\frac{-f_0 p_m}{V_0^2}(1-k)} \frac{n_0'^2}{V_0^2} g \cdot \frac{Wd}{2a} \quad \ldots \quad (23)$$

The stress in the sheet can be found from equations (22) and (23) if the density is known. With a specific gravity of ϱ the density will be $62 \cdot 5\varrho$ lb/cu ft.

From equation (22) the thickness $h = \frac{m}{62 \cdot 5\varrho}$ ft.

The stress $= \frac{T}{h}$ lb/sq ft ,

$$= \frac{62 \cdot 5}{144} \cdot \frac{T}{m} \cdot \varrho \text{ lb/sq in.,}$$

$$= 0 \cdot 434 \frac{1}{\left(\frac{-f_0 p_m}{V_0^2}\right)^2} \cdot \frac{n_0'^2}{V_0^2} \cdot g \cdot d^2 \quad \ldots \quad (24)$$

The acceleration-penetration curves for different values of k are shown in Fig. 7, the numerical values and corresponding masses, tensions and stresses in the sheet are given in Table 2.

APPENDIX II

Determination of Equations of Motion of an Aircraft Landing on an Infinite Sheet under Transverse Tension

It is shown in section 2 that if a portion of the sheet is constrained to move laterally with a velocity V the force exerted by the sheet is given in equation (2) by

$$2\sqrt{\left(\frac{Tm}{g}\right)}\,.\,V \text{ lb/ft run},$$

$$= 2W\lambda V \text{ lb/ft run}. \qquad \qquad (25)$$

By taking a definite shape of the keel the total force on the aircraft at any instant can be calculated.

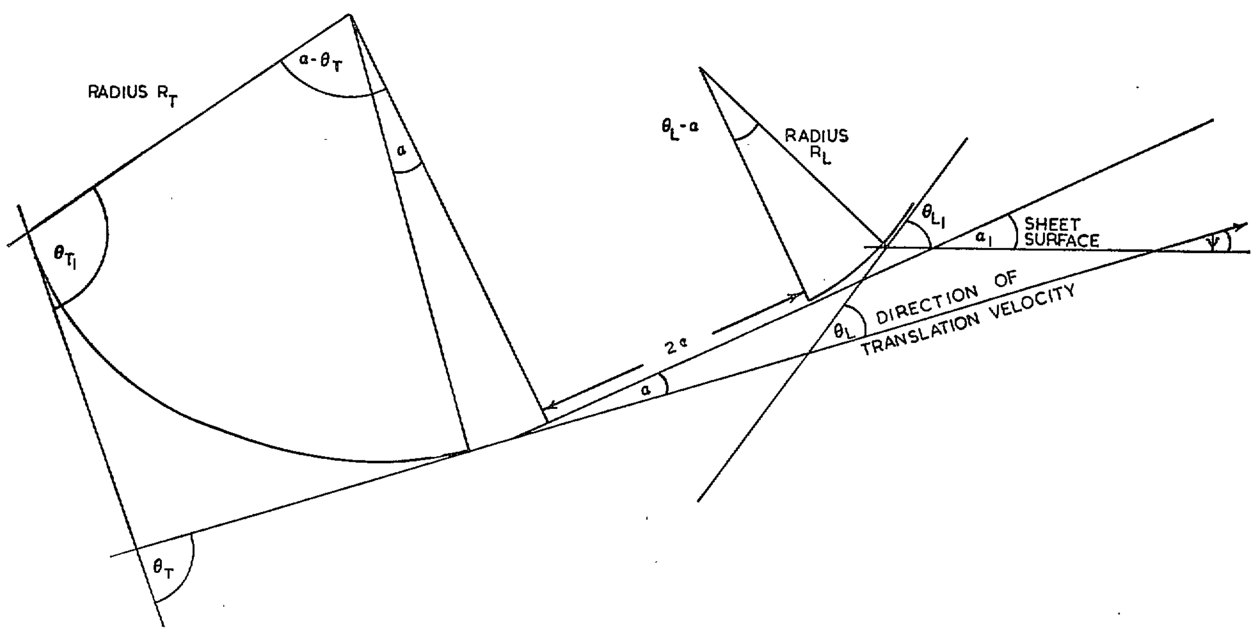

FIG. 2.

Suppose the aircraft makes contact with the sheet along a keel which consists of a central portion of length $2e$ with radii R_T at the tail and R_L at the nose. Fig. 2 shows the attitude of the keel after it has penetrated the sheet.

Let	V	=	Linear velocity of c.g. of aircraft,
	$\dot{\alpha}_1$		Angular velocity about c.g.,
	ψ		Angle V makes with the horizontal,
	α		Angle straight portion of keel makes with V,
	θ_L		Angle tangent at point of entry of nose makes with V,
	θ_T		Angle tangent at point of exit of tail makes with V,
	$\alpha_1,\ \theta_{L1},\ \theta_{T1}$		Angles with horizontal corresponding to α, θ_L, θ_T respectively,

$$\left.\begin{aligned} \text{therefore}\quad \alpha_1 &= \alpha + \psi \\ \theta_{L1} &= \theta_L + \psi \\ \theta_{T1} &= \theta_T + \psi \end{aligned}\right\}, \qquad (26)$$

θ direction of the tangent at any point on the keel relative to the direction of V.

If θ is positive that point on the keel is entering the sheet and if θ is negative it is leaving the sheet.

The force of the sheet is given by equation (25) for points entering the sheet and is zero for points leaving the sheet. Consequently if $\theta_T > 0$ a force will be applied on the whole of the tail, but if $\theta_T < 0$, there will be no force exerted on the tail aft of the point $\theta = 0$. Now on initial contact $\theta_{IT} = 0$ and $\psi < 0$, so that θ_T will be greater than zero and the whole of the tail from $\theta = \theta_T$ to $\theta = \alpha$ will be effective. Generally after a short time, if the aircraft has a horizontal as well as a vertical velocity, $|\theta_{IT}|$ will be greater than $|\psi|$, so that $\theta_T = \theta_{IT} - \psi < 0$, and in this case only the sheet touching the portion of the tail from $\theta = 0$ to $\theta = \alpha$ will be effective.

For the purpose of determining the forces on the aircraft the motion will be referred to moving axes (x_1, x_2, x_3) ; x_1 is in direction V, x_2 is perpendicular to V and upwards, x_3 is horizontal. The origin is taken at the centre of the straight portion of the keel.

The forces due to the sheet will consist of drag D, in negative direction x_1, lift L in direction x_2 and moment M in direction x_3. The air forces in the same directions will be D_A, L_A, M_A. The angular displacement will be in direction x_3.

The moving axes have rotation $\Omega = (0, 0, \dot{\psi})$.

The motion of the aircraft is as follows:—

Translation of c.g. of aircraft.

$$\begin{aligned} &\text{Velocity} &&= (V, 0, 0) \\ &\text{Acceleration} &&= \dot{V} + \Omega_A V = (\dot{V}, V\dot{\psi}, 0) \\ &\text{Total force} &&= (-D - D_A - W\sin\psi, L + L_A - W\cos\psi, 0) \end{aligned}$$

Rotation about c.g.

$$\begin{aligned} &\text{Angular Velocity} &&= (0, 0, \dot{\alpha}_1) = (0, 0, \dot{\alpha} + \dot{\psi}) \\ &\text{Angular acceleration} &&= \ddot{\alpha}_1 + \Omega_A \dot{\alpha}_1 = (0, 0, \ddot{\alpha} + \ddot{\psi}) \\ &\text{Total moment} &&= (0, 0, M + M_A) \end{aligned}$$

Now force = mass $\times$ acceleration and couple = inertia $\times$ angular acceleration, so that

$$\left.\begin{aligned} -D - D_A - W \sin\psi &= \frac{W}{g}\dot{V} \\ -L - L_A - W \cos\psi &= \frac{W}{g} V\dot{\psi} \\ M + M_A &= \frac{I}{g}(\ddot{\psi} + \ddot{\alpha}) \end{aligned}\right\} ; \quad \ldots \ldots \ldots \quad (27)$$

DLM will now be determined in terms of the motion of the aircraft, which is a linear velocity V in direction ψ to the horizontal and an angular velocity $\dot{\alpha} + \dot{\psi}$.

Taking first the translation V without rotation, the normal velocity at point θ is $V \sin \theta$. Hence by equation (25)

Normal force $= 2\lambda W . \; V \sin\theta$ per ft run provided $\theta > 0$.

Consider first the case of $\theta_T > 0$.

Lift $L = \int_{\theta_T}^{\theta_L} (2\lambda W . V \sin\theta) \cos\theta . R . d\theta$,

where $R =$ radius of curvature at point θ.

On integrating separately over tail, straight portion and nose,

$$L = \int_{\theta_T}^{\alpha} 2\lambda W . V \sin\theta \cos\theta \, R_T \, d\theta + \int_{-e}^{e} 2\lambda W . V \sin\alpha \cos\alpha . dz$$
$$+ \int_{\alpha}^{\theta_L} 2\lambda W . V \sin\theta . \cos\theta . R_L . d\theta ,$$

where $R \, d\theta$ is replaced by dz over the straight portion.

Therefore

$$L = \lambda W . V R_T(\sin^2\alpha - \sin^2\theta_T) + 2e \sin 2\alpha + R_L(\sin^2\theta_L - \sin^2\alpha) .$$

Similarly

$$D = \lambda W V[R_T\{(\alpha - \theta_T) - \tfrac{1}{2}(\sin 2\alpha - \sin 2\theta_T)\}$$
$$+ 4e\sin^2\alpha + R_L\{(\theta_L - \alpha) - \tfrac{1}{2}(\sin 2\theta_L - \sin 2\alpha)\}] ,$$

$$M_V = \lambda W V[R_T(\sin^2\alpha - \sin^2\theta_T)\{-(e + \bar{x})\cos\alpha - (R_T - \bar{y})\sin\alpha\}$$
$$+ R_T\{(\alpha - \theta_T) - \tfrac{1}{2}(\sin 2\alpha - \sin 2\theta_T)\}\{(R_T - \bar{y})\cos\alpha - (e + \bar{x})\sin\alpha\}$$
$$- 4e\bar{x}\sin\alpha$$
$$+ R_L(\sin^2\theta_L - \sin^2\alpha)\{(e - \bar{x})\cos\alpha - (R_L - \bar{y})\sin\alpha\}$$
$$+ R_L\{(\theta_L - \alpha) - \tfrac{1}{2}\sin 2\theta_L(\sin 2\alpha)\}\{(R_L - \bar{y})\cos\alpha + (e - \bar{x})\sin\alpha\}] . \quad \ldots \quad (28)$$

For the case $\theta_T < 0$ equations (28) are modified by substituting 0 for θ_T.

The rotation $\omega = \dot{\alpha} + \dot{\psi}$ will produce an appreciable change of moment but it may be assumed that the change of lift and drag will be small and can be neglected.

The transition point, at which the normal velocity is zero, will not be where $\theta = 0$, so let it be at $\theta = \phi$, which will now be determined.

The velocity at the point, $(x, y, 0)$ referred to axes along and at right-angles to the keel with origin at the centre of the keel will be

$$[V \cos \alpha - \omega(y - \bar{y}), \quad - V \sin \alpha + \omega(x - \bar{x}), \quad 0],$$

where $(\bar{x}, \bar{y}, 0)$ are the co-ordinates of the c.g.

At the point $\theta = \phi$ on the tail the co-ordinates are

$$[- e - R_T \sin (\alpha - \phi), \quad R_T \{1 - \cos (\alpha - \phi)\}, \quad 0].$$

The normal velocity is zero if $\tan (\alpha - \phi) = - \dfrac{V_y}{V_x}$,

therefore
$$\tan (\alpha - \phi) = \frac{V \sin \alpha + \omega\{e + R_T \sin (\alpha - \phi) + \bar{x}\}}{V \cos \alpha - \omega\{R_T[1 - \cos (\alpha - \phi)] - \bar{y}\}},$$

which reduces to

$$\tan (\alpha - \phi) = \frac{V \sin \alpha + \omega(e + \bar{x})}{V \cos \alpha - \omega(R_T - \bar{y})}.$$

The two cases to be considered are $\theta_T > \phi$ for the initial motion and $\theta_T < \phi$ for the motion after a short time.

The normal velocity over the length of tail $\theta = 0$ to $\theta = \phi$ is due to a combination of the velocity V and angular velocity ω and will be fairly small, and the contribution to the moment will be small. To facilitate the computation it will be assumed that it can be neglected.

By neglecting this portion the moment on the aircraft due to translation of the c.g. and rotation about the c.g. is given in two terms, one depending on the translation velocity only and the other depending on the rotation only. The translation effects are given in equations (28); the effect of rotation will now be determined.

The normal velocities on the nose, straight portion and tail for a rotation about the c.g. will be:—

Normal velocity on nose

$$= - (\dot{\alpha} + \dot{\psi})\{(e - \bar{x}) \cos (\theta - \alpha) + (R_L - \bar{y}) \sin (\theta - \alpha)\}.$$

Normal velocity on straight portion

$$= - (\dot{\alpha} + \dot{\psi})(x - \bar{x}).$$

Normal velocity on tail

$$= (\dot{\alpha} + \dot{\psi})\{(e + \bar{x}) \cos (\alpha - \theta) + (R_T - \bar{y}) \sin (\alpha - \theta)\}.$$

Using these velocities and applying equation (25), the moment due to rotation (M_ω) is given by

$$\begin{aligned} M_\omega = & - W\lambda(\dot{\alpha} + \dot{\psi})[R_L\{(e - \bar{x})^2 + (R_L - \bar{y})^2\}(\theta_L - \alpha) \\ & + R_L\{(e - \bar{x})^2 - (R_L - \bar{y})^2\} \tfrac{1}{2} \sin 2 (\theta_L - \alpha) \\ & + R_L(e - \bar{x}) (R_L - \bar{y})\{1 - \cos 2 (\theta_L - \alpha)\} \\ & + \tfrac{4}{3}e(e^2 + 3\bar{x})^2 \\ & + R_T\{(e + \bar{x})^2 + (R_T - \bar{y})^2\}(\alpha - \theta_T) \\ & + R_T\{(e + \bar{x})^2 - (R_T - \bar{y})^2\} \tfrac{1}{2} \sin 2 (\alpha - \theta_T) \\ & + R_T(e + \bar{x}) (R_T - \bar{y})\{1 - \cos 2 (\alpha - \theta_T)\}] \qquad \ldots \qquad (29) \end{aligned}$$

for $\theta_T > 0$; when $\theta_T < 0$ substitute $\theta_T = 0$ in equation (29).

Equation (27) can now be written in the form

$$\left.\begin{aligned} \frac{\dot{V}}{g} &= - \sin\psi - \lambda V d - d_A \\ \frac{V\dot{\psi}}{g} &= - \cos\psi + \lambda V \, . \, l + l_A \\ \frac{I(\ddot{\alpha} + \ddot{\psi})}{Wg} &= \lambda V \, . \, m_v + \lambda(\dot{\psi} + \dot{\alpha})m_\omega + m_A \end{aligned}\right\} , \qquad \ldots \qquad (30)$$

where $d = \dfrac{D}{\lambda VW}$, $l = \dfrac{L}{\lambda VW}$, $m_v = \dfrac{M_v}{\lambda VW}$, $m_\omega = \dfrac{M_\omega}{\lambda W(\dot{\alpha} + \dot{\psi})}$,

$d_A = \dfrac{D_A}{W}$, $l_A = \dfrac{L_A}{W}$, $m_A = \dfrac{M_A}{W}$.

In equation (30) the first equation gives the drag acceleration of the whole aircraft and the second gives the normal acceleration.

To assist in the computation the sheet forces have been determined in terms of the angles of incidence of various parts of the aircraft with the sheet. The important parameters on penetration are the depth of penetration of the c.g. (p) and the rotation of the c.g. from the horizontal ($\alpha + \psi$). To determine the vertical velocity $V \sin\psi$ in terms of the penetration, p must be found in terms of α, θ_L, θ_T, ψ.

If p is measured vertically downwards

$$\begin{aligned} p = & \{R_L(\cos \alpha - \cos \theta_L) + (e - \bar{x}) \sin \alpha\} \cos \psi \\ & + \{R_L(\sin \theta_L - \sin \alpha) + (e - \bar{x}) \cos \alpha\} \sin \psi \, . \qquad \ldots \qquad (31) \end{aligned}$$

Hence the vertical velocity $= - \dfrac{dp}{dt}$.

Therefore $$\frac{dp}{dt} = -V \sin \psi ,$$

therefore $$p_0 - p = \int_0^t (V \sin \psi)\, dt . \qquad \text{(32)}$$

Equations (30), (31) and (32) are solved by successive approximation.

For the usual small angles of incidence of the keel with the sheet on touching down the retardation will be negligible during the short time it takes for the whole of the straight portion to make contact with the sheet ; equations (28) and (29) hold after the condition has arisen and can be applied.

If the aircraft is landing nose up ($\alpha_1 > 0$), $t = 0$ is chosen when $\theta_{1L} = \alpha_1$, and if the aircraft is landing nose down ($\alpha_1 < 0$), $t = 0$ is chosen when $\theta_{1T} = \alpha_1$; these conditions are illustrated in Fig. 3.

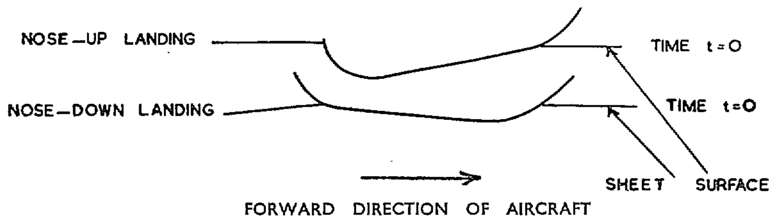

FIG. 3.

The successive approximation is as follows:—

From the geometry of the aircraft and its motion on touch down V_0, ψ_0, $\alpha_0 + \psi_0$, $\dot{\alpha}_0 + \dot{\psi}_0$, p_0, are known at $t = 0$.

Hence d_0, l_0, m_{v0}, $m_{\omega 0}$, d_A, l_A, m_A can be calculated.

Using equation (30) $\dot{V}_0$, $\dot{\psi}_0$, $(\ddot{\psi} + \ddot{\alpha})_0$ are determined at $t = 0$.

By taking a sufficiently short increment of time the values $\dot{V}_0$, $\dot{\psi}_0$, $(\ddot{\psi} + \ddot{\alpha})_0$ may be assumed to remain unaltered, so that

$$V_1 - V_0 \simeq \dot{V}_0 \, . \, t_1 . \qquad \text{(33)}$$

Hence at time $t = t_1$, V_1, ψ_1, $(\dot{\psi} + \dot{\alpha})_1$, $(\psi + \alpha)_1$ are determined.

Also using equation (32) p_1 is determined.

The process is repeated to determine $\dot{V}_1$, $\dot{\psi}_1$, $(\ddot{\psi} + \ddot{\alpha})_1$, and hence V_2, ψ_2, $(\dot{\psi} + \dot{\alpha})_2$ $(\psi + \alpha)_2$, and so on.

In practice the increments of time may be only moderately small, and a correction is made to equation (33) by taking the values of V, ψ , $\psi + \alpha$, $\dot{\psi} + \dot{\alpha}$, p at times t_1, t_2, t_3, t_4 ...... where $t_1 = 0 = t_2 - t_1 = t_3 - t_2 = t_4 - t_3 =$ ...... and is small.

The following more accurate equation is used in place of equation (33):

$$\frac{V_n - V_n - 2}{2t_1} = \dot{V}_{n-1} . \qquad \text{(34)}$$

APPENDIX III

Method of Computation

An attempt to solve equations (30), (31) and (32) directly by the successive approximation given in Appendix II is very laborious as it necessitates solving five trigonometrical equations for each increment of time. A much simpler process is possible by using graphical methods.

Equations (28) and (29) give l, d, m_v, m_ω and p in terms of α, θ_L, θ_T, e, R_L, R_T.

As an illustration a typical shape of keel is taken by putting

$$R_T = 30 \text{ ft}, \qquad \bar{x} = 0\cdot5 \text{ ft},$$

$$R_L = 20 \text{ ft}, \qquad \bar{y} = 2 \text{ ft},$$

$$2e = 10 \text{ ft}.$$

With these values and $\theta_T > 0$,

$$\left.\begin{aligned}
d &= 10\left[\alpha - \tfrac{1}{2}\sin 2\alpha + 2\sin^2\alpha - 3\left(\theta_T - \tfrac{1}{2}\sin 2\theta_T\right) + 2\left(\theta_L - \tfrac{1}{2}\sin 2\theta_L\right)\right], \\
l &= 10\left[\sin^2\alpha + \sin 2\alpha - 3\sin^2\theta_T + 2\sin^2\theta_L\right]. \\
m_v &= 10\left[-49\sin\alpha + \alpha(48\cos\alpha - 25\cdot5\sin\alpha) - \theta_T(84\cos\alpha - 16\cdot5\sin\alpha)\right. \\
&\quad + \theta_L(36\cos\alpha + 9\sin\alpha) + \sin\theta_T\{84\cos(\alpha - \theta_T) - 16\cdot5\sin(\alpha - \theta_T)\} \\
&\quad \left. - \sin\theta_L\{36\cos(\theta_L - \alpha) - 9\sin(\theta_L - \alpha)\}\right], \\
m_\omega &= -10\left[17\cdot2 + 688(\theta_L - \alpha) - 304\sin 2(\theta_L - \alpha) + 324\sin^2(\theta_L - \alpha)\right. \\
&\quad \left. + 2442(\alpha - \theta_T) - 1131\sin 2(\alpha - \theta_T) + 924\sin^2(\alpha - \theta_T)\right], \\
p &= 20\left[\cos(\alpha + \psi) - \cos(\theta_L + \psi) + 4\cdot5\sin(\alpha + \psi)\right].
\end{aligned}\right\} \quad \ldots \quad (35)$$

For values of $\theta_T < 0$ substitute $\theta_T = 0$ in equation (35).

The values of d, l, m_v, m_ω are plotted against θ_L for different values of α with $\theta_T = 0$ in Figs. 13 to 16; p is plotted against $(\theta_L + \psi)$ for different values of $(\alpha + \psi)$ in Fig. 17. The components of d, l, m_v, m_ω due to the terms in θ_T are plotted against θ_T for different values of α in Figs. 18 to 21; this component is only used for the very short time in which $\theta_T > 0$. The value of p is plotted against $(\theta_T + \psi)$ for different values of $(\alpha + \psi)$ in Fig. 22.

The air forces d_A, l_A, m_A will be dependent on α, V only.

Below the stalling speed

$$l_A \simeq \frac{3}{4}\left(\frac{V}{V_s}\right)^2,$$

$$d_A \simeq \frac{1}{5}\cdot l_A.$$

Above the stall

$$l_A = \frac{V^2\alpha}{V_s^2\alpha_s},$$

$$d_A \simeq \frac{1}{5} \cdot l_A .$$

m_A will depend on the trim of the aircraft, and for the lack of more accurate information has been assumed to be zero.

For landings just above the stall no serious error will be introduced in determining the maximum accelerations and penetrations by assuming the weight of the aircraft as reacted by the air forces, although the subsequent motion may be seriously affected and the estimate of the velocity of rebound would be conservative.

If the forward velocity on landing is small it would be sufficiently accurate to assume that the air forces were zero.

By using the graphs plotted from equations (35) the subsequent solution of equations (30), (31) and (32) for any particular condition of landing is very rapid. In considering the conditions of landing the tension and mass of the sheet are included as well as the velocity and attitude of the aircraft.

TABLE 1

Acceleration against Penetration in an Infinite Landing Sheet for Various Ratios of Maximum to Initial Contact Length—Gravity Forces Absent

$$\frac{f}{f_0} = \frac{f}{2\lambda a V_0 g} = \left[\left(1 + \frac{p}{V_0/2\lambda a g}\,\frac{bV_0}{2\lambda a^2 g}\right)\left\{1 - \frac{p}{V_0/2\lambda a g}\left(1 + \tfrac{1}{2}\,\frac{p}{V_0/2\lambda a g}\,\frac{bV_0}{2\lambda a^2 g}\right)\right\}\right]$$

from equation (6)

$\dfrac{p}{V_0/2\lambda a g}$	Values of $f/2\lambda a V_0 g$							
	$bV_0/2\lambda a^2 g$							
	0	1	2	3	4	6	12	24
0	1	1	1	1	1			
0·1	0·9	0·9845	1·068	1·1505	1·232			
0·2	0·8	0·936	1·064	1·184	1·296			
0·3	0·7	0·8515	0·976	1·0735	1·144			
0·4	0·6	0·728	0·792	0·792	0·728			
0·5	0·5	0·5625	0·500	0·3125	0			
0·6	0·4	0·352	0·088	—	—			
0·7	0·3	0·0935	—	—	—			
0·8	0·2	—	—	—	—			
0·9	0·1	—	—	—	—			
1·0	0	—	—	—	—			

	$bV_0/2\lambda a^2 g$							
	0	1	2	3	4	6	12	24
$\dfrac{\text{Maximum contact length}}{\text{Initial contact length}}$	1	1·732	2·236	2·646	3	3·605	5	7
f_m/f_0	1	1	1·076	1·188	1·299	1·504	2·005	2·751
Efficiency, per cent	50	68·3	75·2	76·7	77	76·54	74·85	72·7

TABLE 2

Acceleration against Penetration in an Infinite Landing Sheet with Constant Contact Length and Various Ratios of Gravity and Air Forces to Sheet Forces

$$\frac{f_0}{V_0^2}\,p = (1-k)^2\left[1 - \frac{f}{f_0} - \frac{k}{1-k}\log f/f_0\right] \quad \text{(equation (19))}$$

Values of pf_0/V_0^2

$\frac{f}{f_0}$	k = 0	0·1	0·15	0·2	0·25
0	1	1	1	1	1
0·1	0·9	0·936	0·946	0·94	0·937
0·2	0·8	0·793	0·785	0·771	0·751
0·3	0·7	0·675	0·661	0·640	0·620
0·4	0·6	0·569	0·551	0·529	0·509
0·5	0·5	0·467	0·451	0·430	0·411
0·6	0·4	0·370	0·355	0·337	0·320
0·7	0·3	0·275	0·263	0·249	0·235
0·8	0·2	0·182	0·173	0·163	0·154
0·9	0·1	0·091	0·086	0·081	0·076
1·0	0	0	0	0	0

	k = 0	0·1	0·15	0·2	0·25
fp_m/V_0^2	0·619	0·637	0·649	0·663	0·681
Efficiency, per cent	80·8	78·5	77·0	75·5	73·4
$\dfrac{m}{W/cd_0}$	0·309	0·354	0·382	0·414	0·454
$\dfrac{T}{\frac{n_0'^2}{V_0^2}\,g\,\frac{Wd_0}{c}}$	0·808	0·872	0·907	0·943	0·979
$\dfrac{\text{Stress}}{\frac{n_0'^2}{V_0^2}\,gd_0^2\varrho}$	1·133	1·070	1·028	0·987	0·937

TABLE 3

Comparison of Aircraft Weights and Fuselage Lengths

Name of Aircraft	Type	Gross Weight (lb)	Length ft	Length in.
Bristol Type 167 Mk. I	Civil	279,000	177	0
Saro S.R./45		290,000	146	0
Avro Lancastrian		65,000	76	10
Avro Tudor I		78,000	79	6
Avro Tudor II		80,000	105	7
Avro York		71,000	78	0
Handley Page Halton		65,000	73	7
Short Sandringham		56,000	86	3
Short Shetland		130,000	108	0
Short Solent		75,000	89	6½
Blackburn Firebrand	Naval	15,671	38	11
De Havilland Sea Hornet		15,682	36	8
Fairey Firefly IV		15,615	37	11
Fairey Spearfish I		21,600	44	7
Hawker Sea Fury X		12,030	34	7
Short Sturgeon I		21,700	44	0
Supermarine Seafire 47		10,200	34	4
Supermarine Seafang 32		10,450	33	6½
De Havilland Vampire I	Jet Propelled	8,578	30	9
Gloster Meteor IV		14,460	41	0
Supermarine E.10/44		No data available	37	6
De Havilland D.H.108		No data available	26	9½
Hawker Tempest VI	Military	12,250	33	10½
De Havilland Mosquito 34		20,000	41	6
Westland Welkin IIA		21,892	44	1
Bristol Brigand I		38,200	46	5
Percival Prentice I	Trainer	3,790	31	3
Fairey Firefly Trainer I		12,300	37	7¼
Supermarine Spitfire Trainer VIII		7,400	31	4½
Reid & Sigrist Desford I		3,300	25	6
Airspeed Consul	Feeder Transport	8,250	35	4
Bristol Wayfarer		37,000	68	4
De Havilland Dove		8,500	39	4
Miles Aerovan		5,400	34	8
Miles Marathon		16,500	52	1
Avro XIX		10,400	42	3
Vickers Armstrong Viking IB		34,000	65	2
Avro Lincoln II	Heavy Military	75,000	78	8½
Handley Page Hastings		75,000	81	3

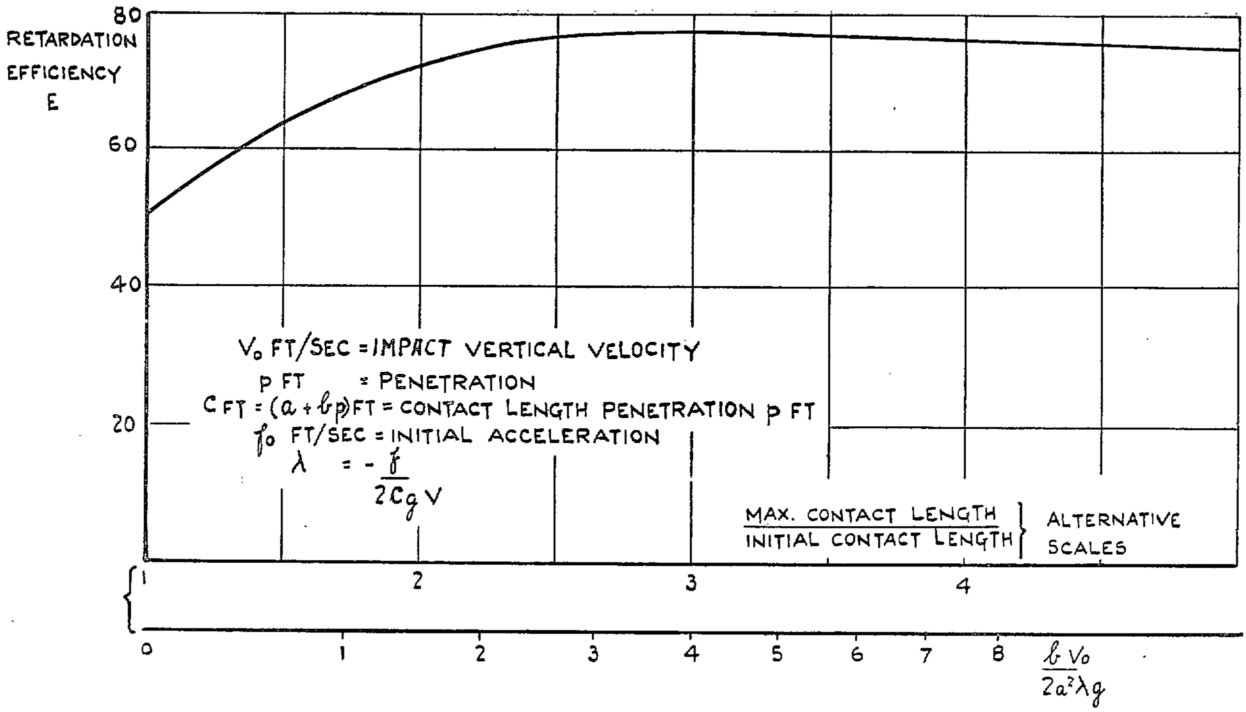

FIG. 4. Retardation efficiency for different linear rates of increase of contact length of keel.

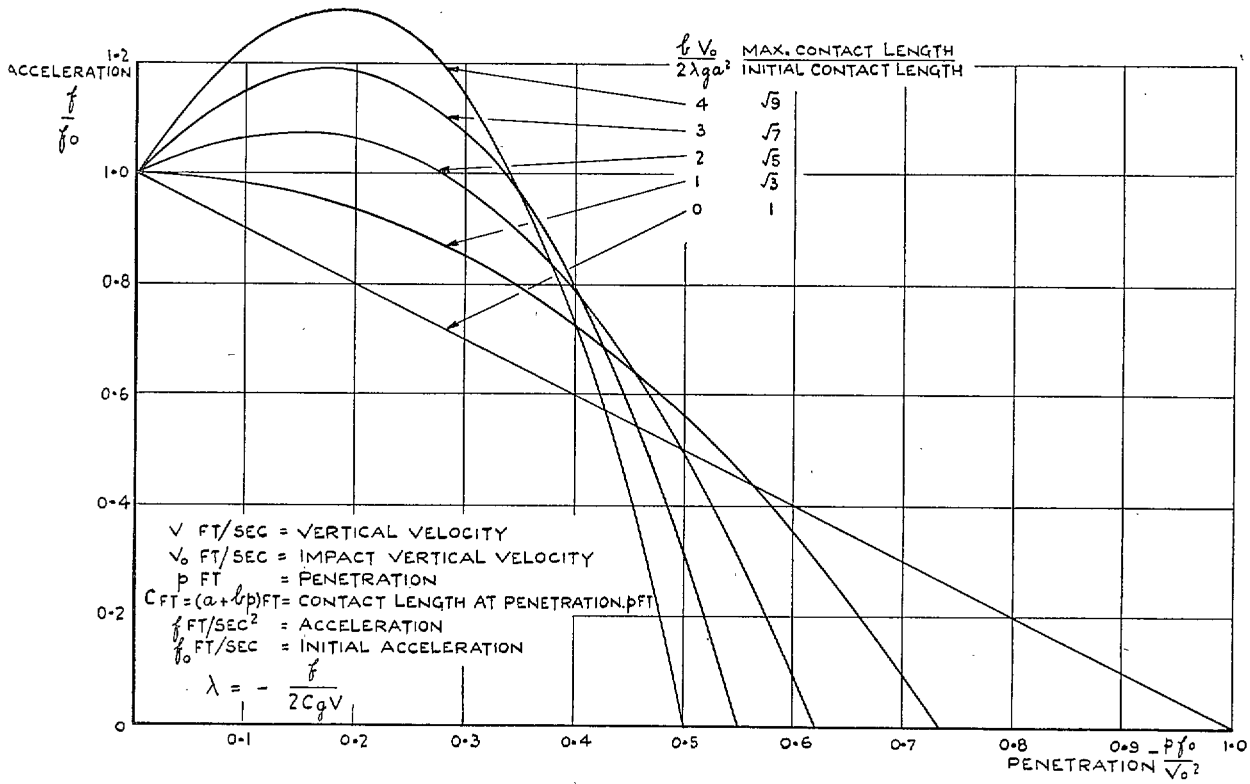

FIG. 5. Vertical acceleration *vs.* penetration curves. Retardation by inertia forces only. Contact length increasing linearly with penetration.

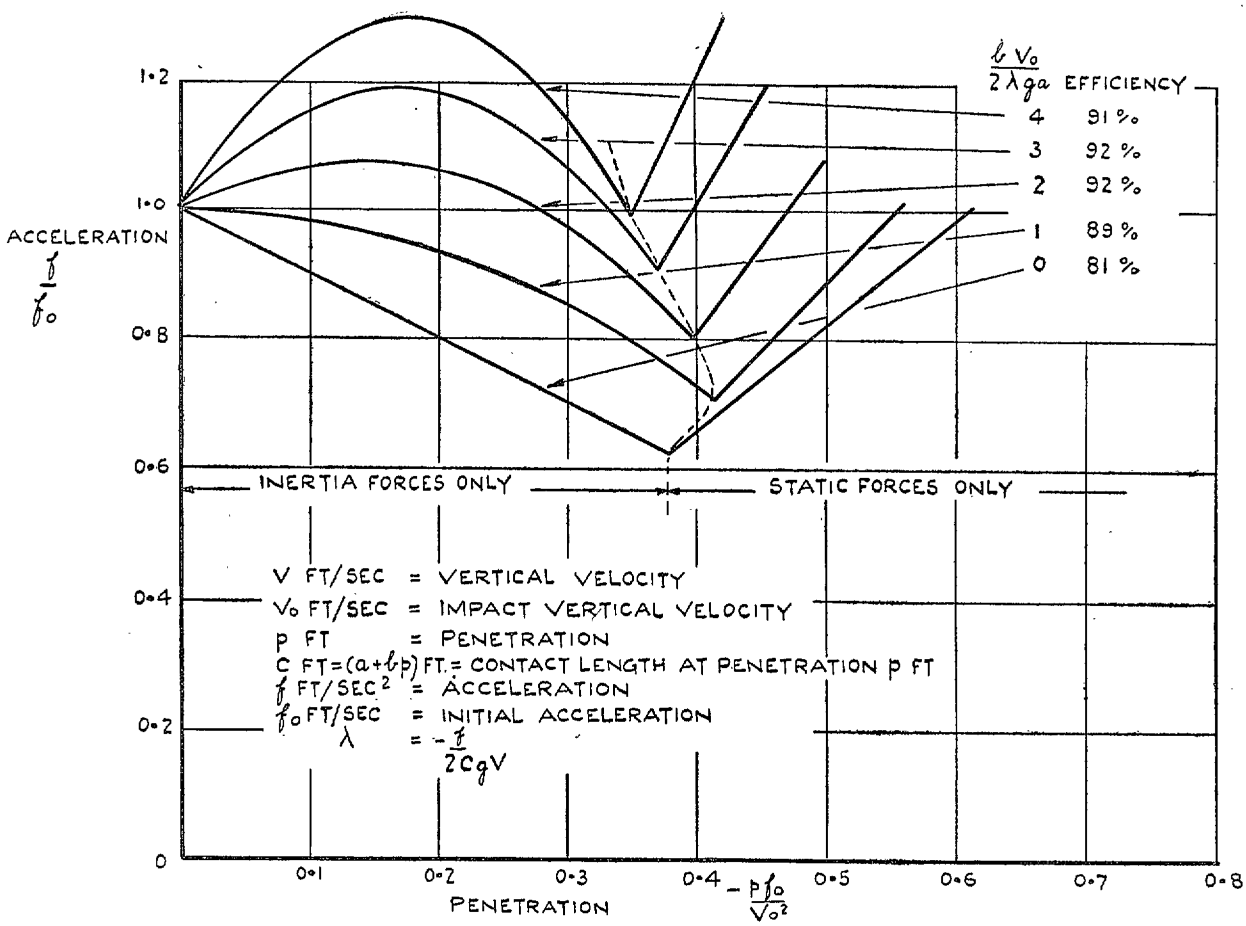

FIG. 6. Vertical acceleration *vs*. penetration curves. Retardation by inertia and static forces. Contact length increasing linearly with penetration.

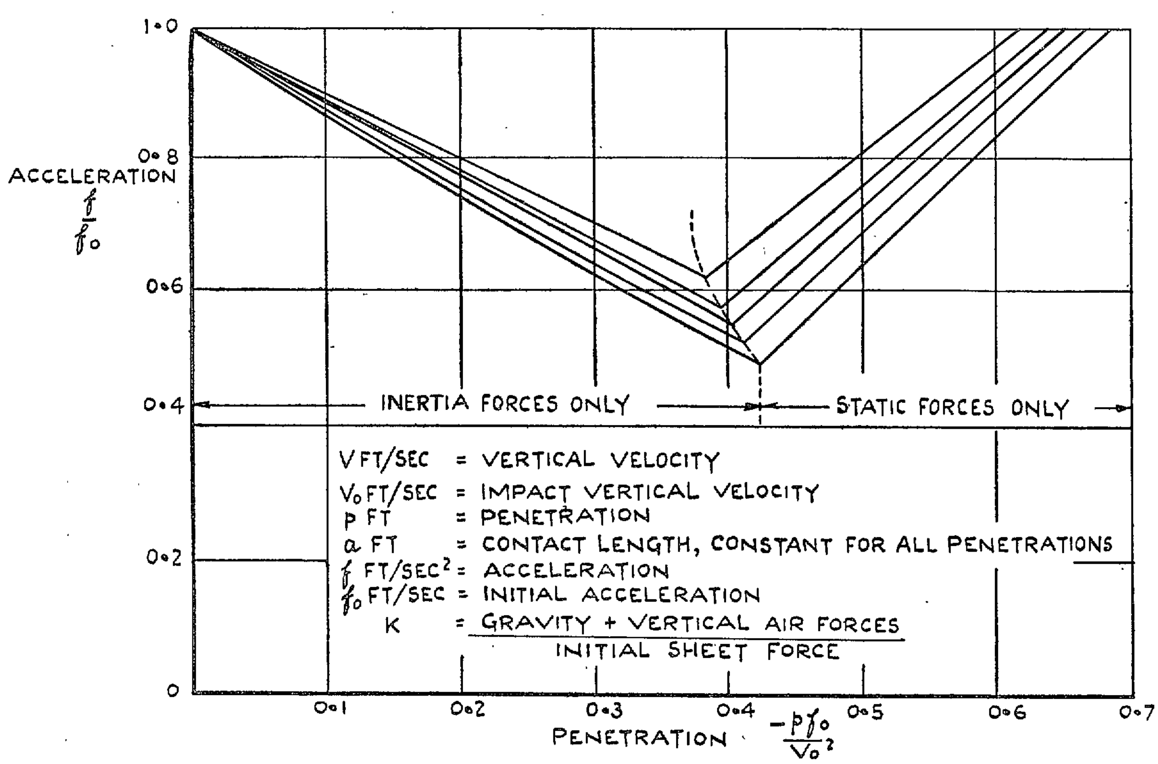

FIG. 7. Vertical acceleration *vs*. penetration curves for different ratios of gravity plus air forces to landing sheet forces. Contact length constant with penetration.

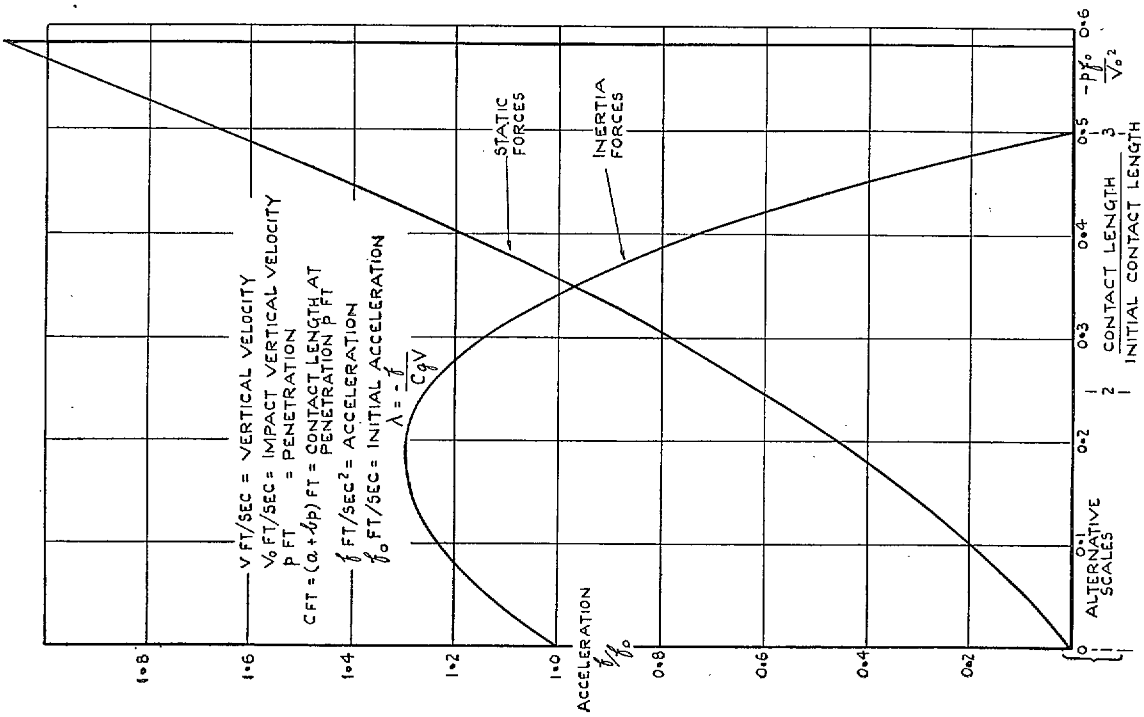

FIG. 8. Vertical acceleration *vs.* penetration curves for retardation by means of inertia and static forces taken separately.

Condition $\frac{bV_0}{2\lambda g a^2} = 4$ in Fig. 4.

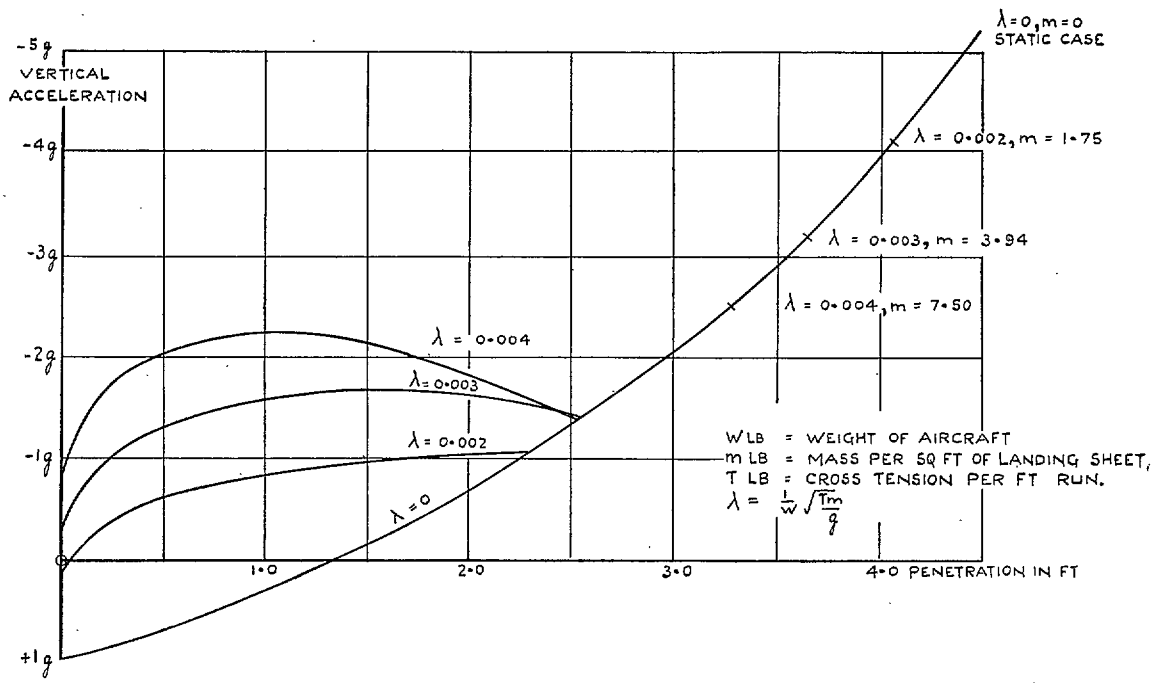

FIG. 9. Vertical acceleration, with penetration. Numerical example of Appendix III. Cross tension 3600 lb/ft. Weight of aircraft 7000 lb. Horizontal velocity zero. Initial vertical velocity 20 ft/sec.

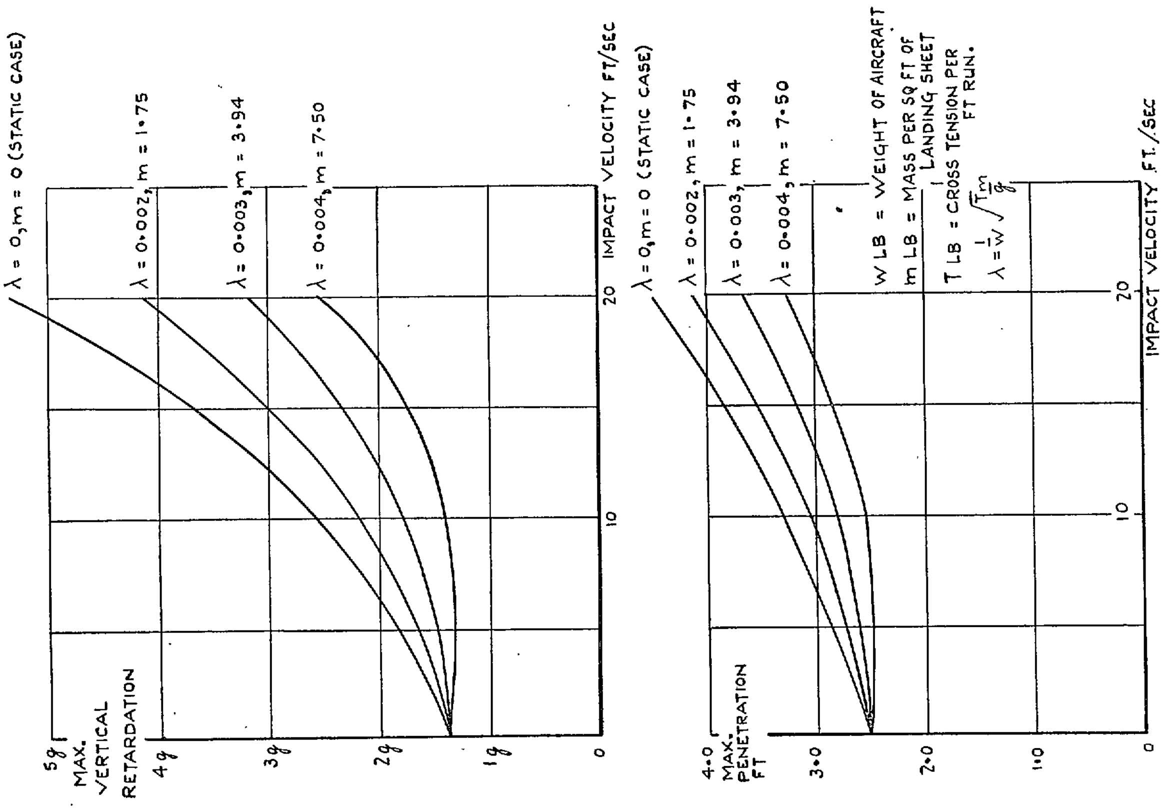

FIG. 10. Maximum accelerations and penetrations *vs.* vertical descent. Numerical example of Appendix III. Cross tension 3600 lb/ft. Weight of aircraft 7000 lb.

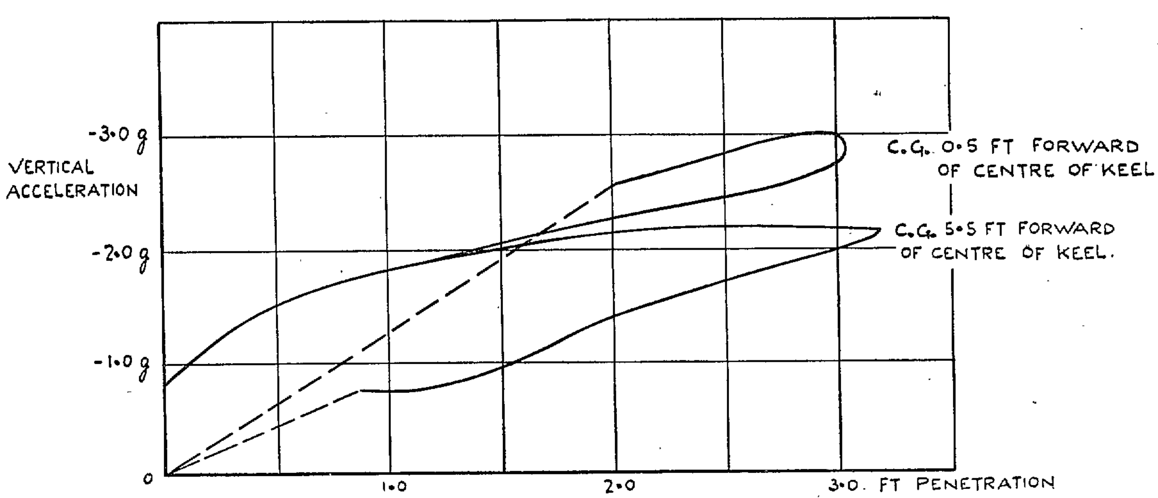

FIG. 11. Vertical acceleration *vs.* penetration with c.g. position. Numerical example of Appendix III. Cross tension 3600 lb/ft. Weight of aircraft 7000 lb. Landing sheet 1·75 lb/sq ft. Initial horizontal velocity 160 ft/sec. Initial vertical velocity 20 ft/sec.

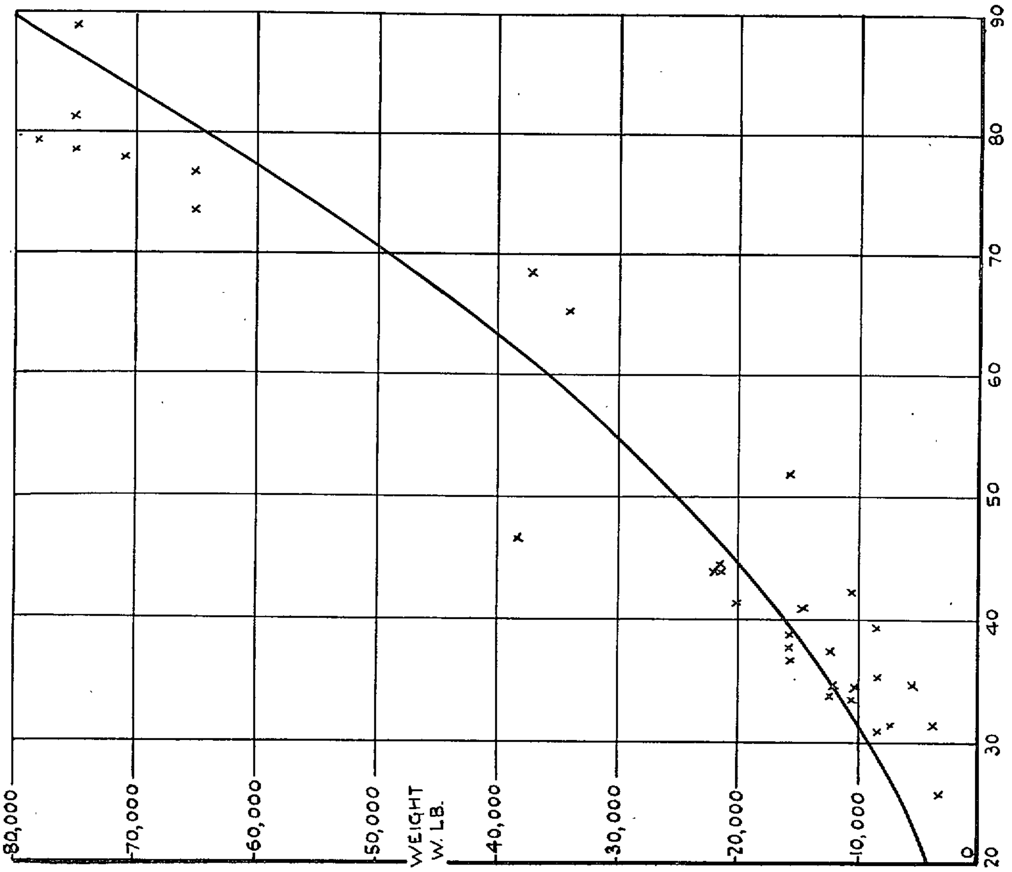

FIG. 12. Variation of aircraft weight with fuselage length.

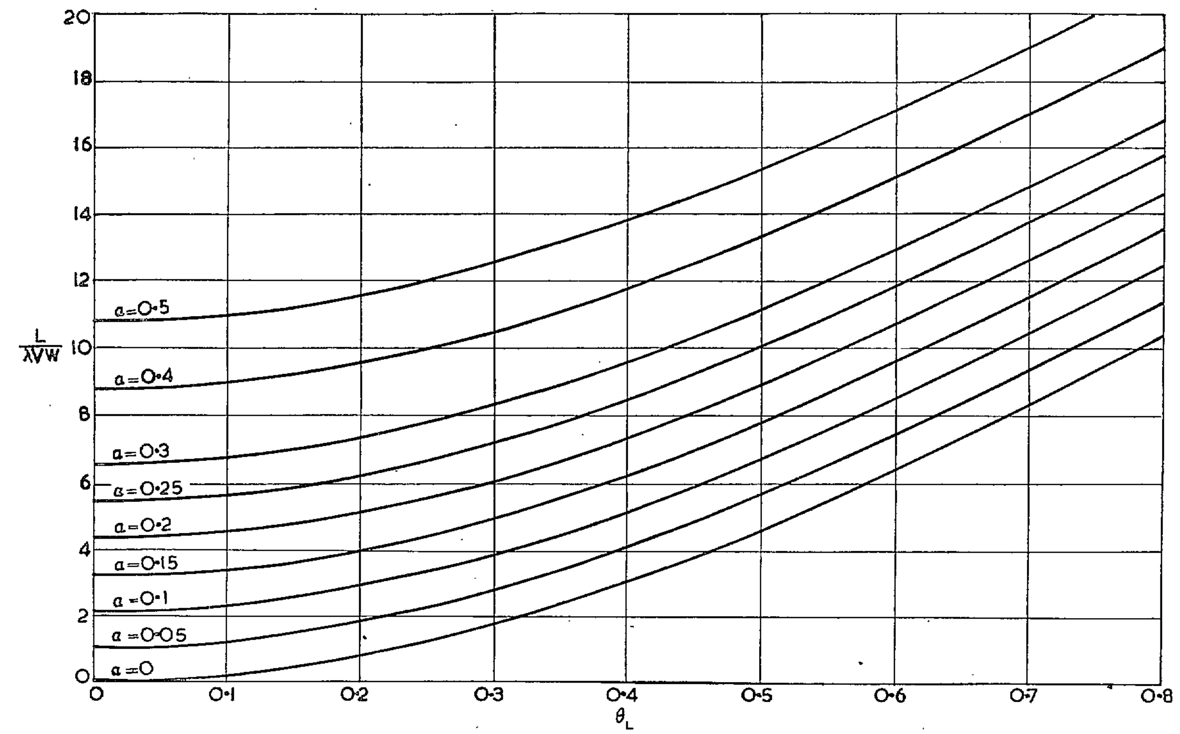

FIG. 13. Variation of ratio of lift to velocity ($L/\lambda VW$) with angles of incidence of nose (θ_L) and central portion of keel (α) ; incidence of stern (θ_T) negative. Numerical example of Appendix III.

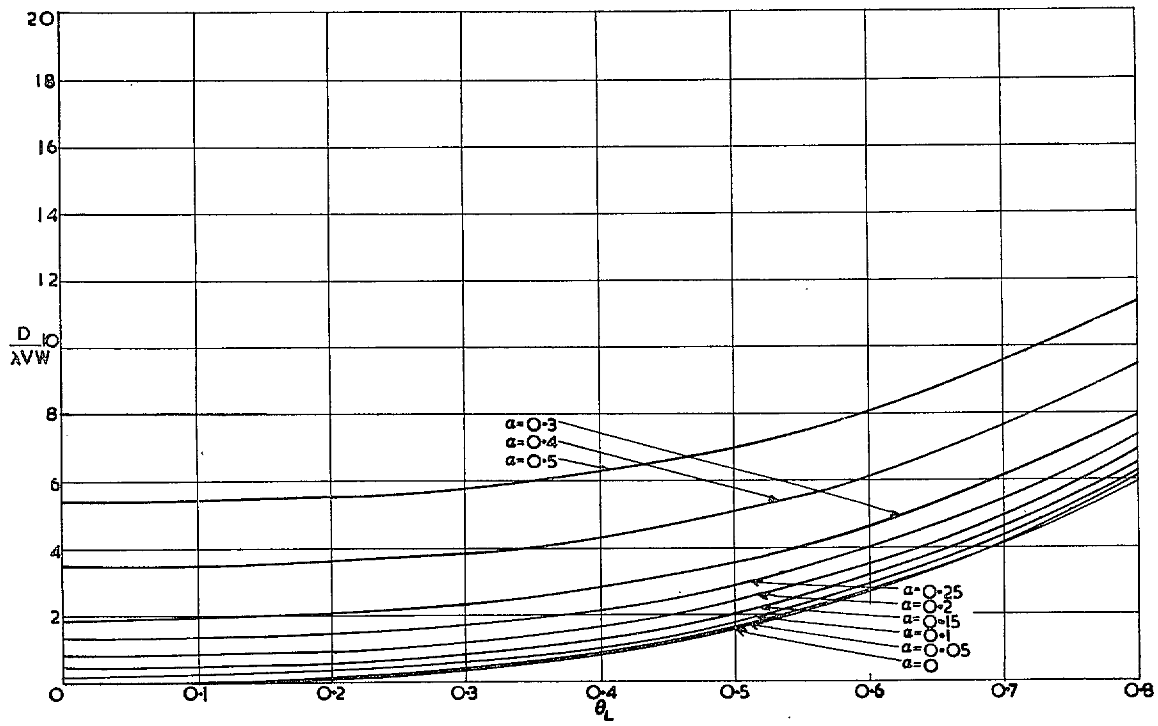

FIG. 14. Variation of ratio of drag to velocity ($D/\lambda VW$) with angles of incidence of nose (θ_L) and central portion of keel (α) ; incidence of stern (θ_T) negative. Numerical example of Appendix III.

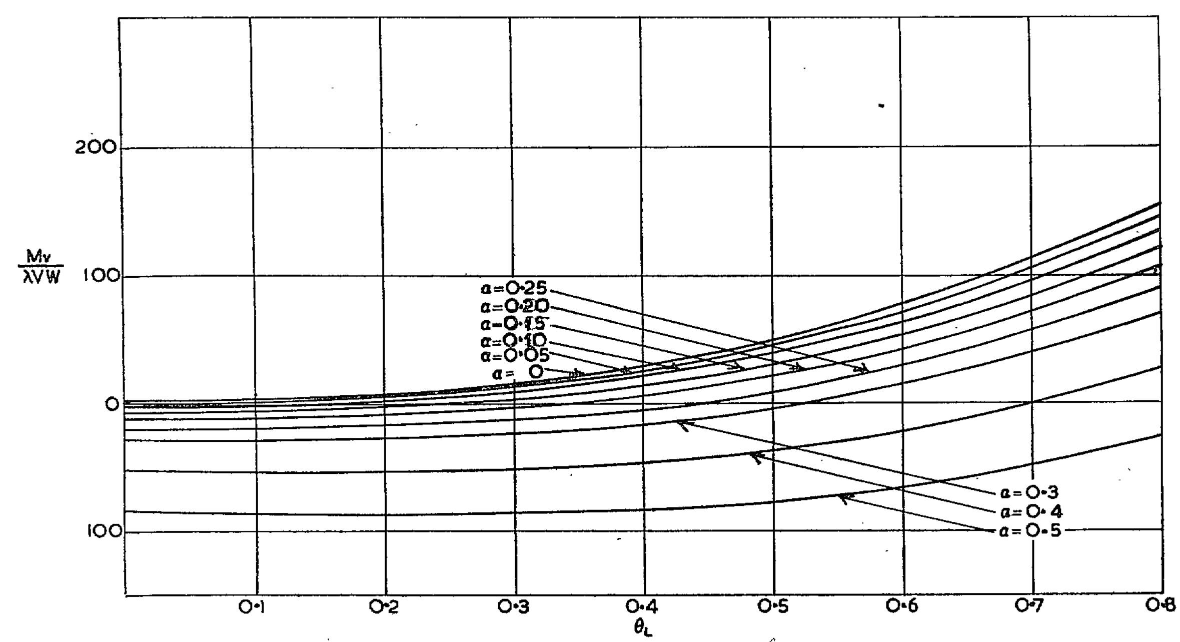

FIG. 15. Variation of ratio of nose-up pitching moment to velocity ($M_v/\lambda VW$) with angles of incidence of nose (θ_L) and central portion of keel (α) ; incidence of stern (θ_T) negative. Numerical example of Appendix III.

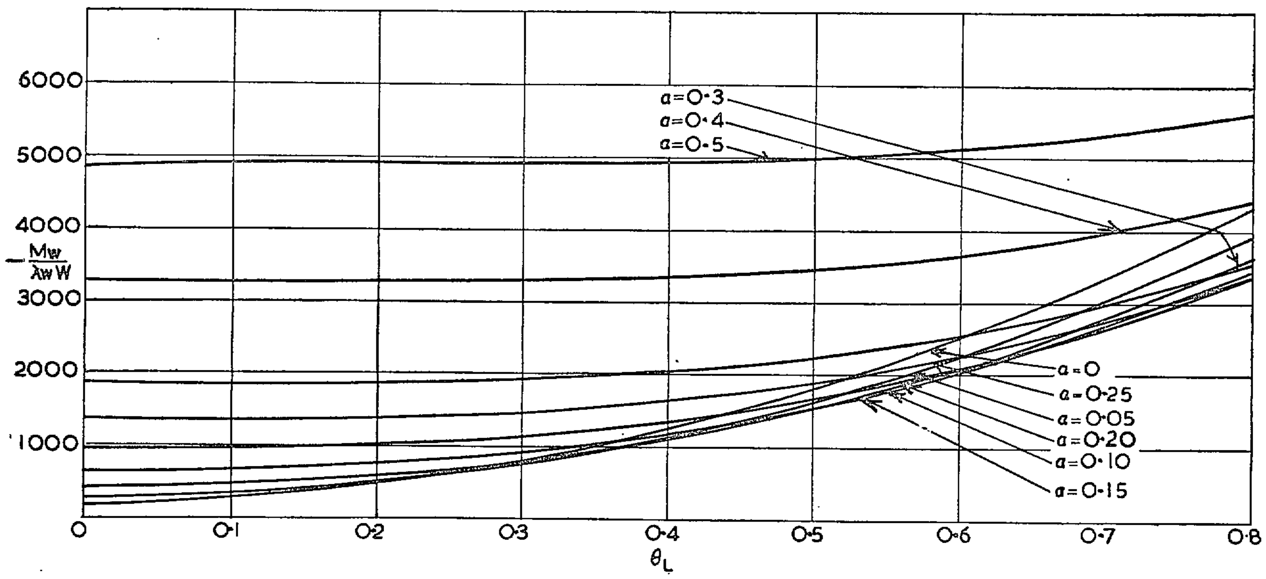

FIG. 16. Variation of ratio of pitching moment to angular velocity ($M_\omega / \lambda_\omega W$) with angles of incidence of nose (θ_L) and central portion of keel (α) ; incidence of stern (θ_T) negative. Numerical example of Appendix III.

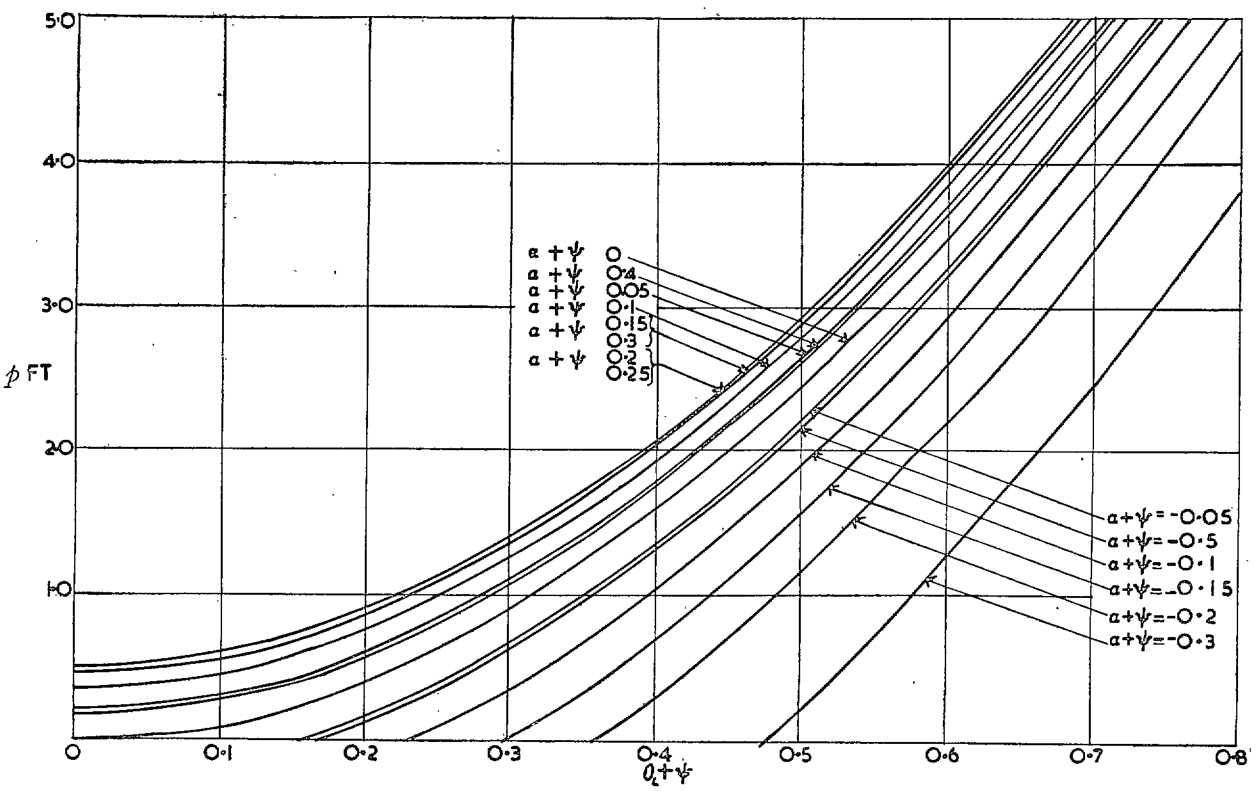

FIG. 17. Variation of penetration (p) with angles to horizontal of nose ($\theta_L + \psi$) and central portion of keel ($\alpha + \psi$). Numerical example of Appendix III.

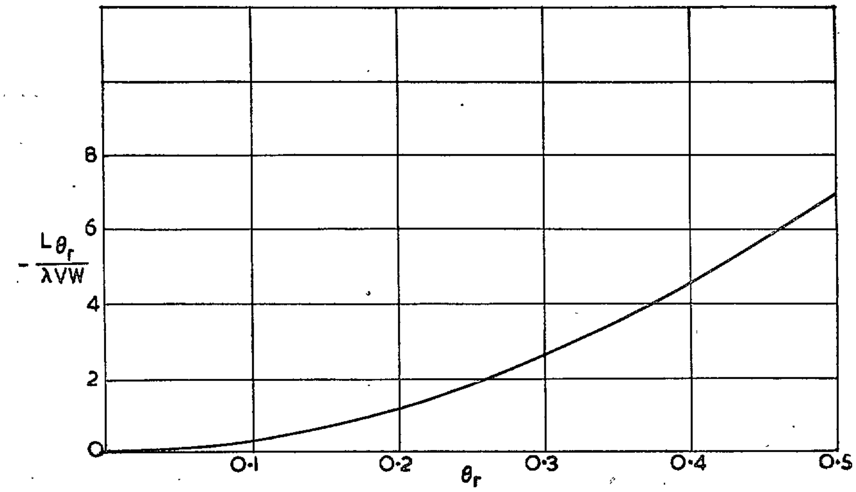

FIG. 18. Component of lift ($L_{\theta T}/VW$) due to a positive angle of incidence at the stern (θ_T). Numerical example of Appendix III.

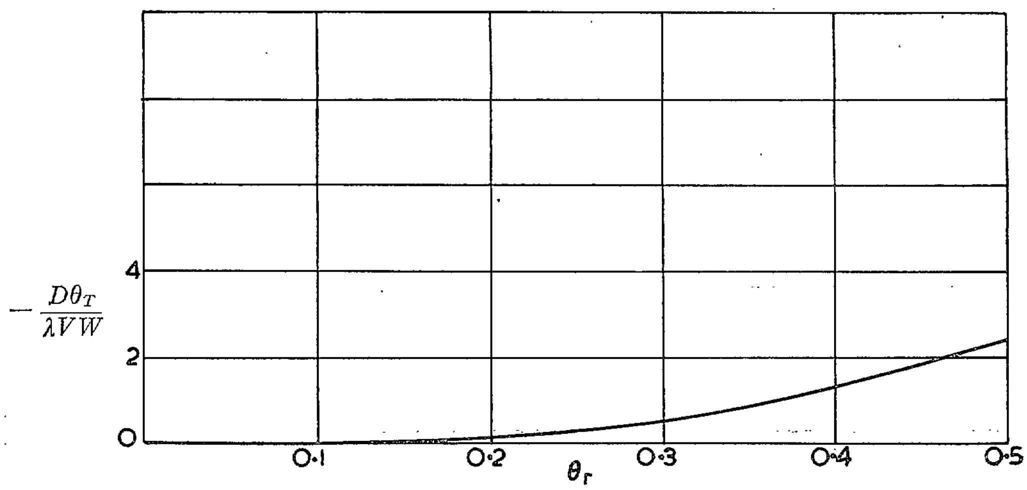

FIG. 19. Component of drag ($D_{\theta T}/\lambda VW$) due to a positive angle of incidence at the stern (θ_T). Numerical example of Appendix III.

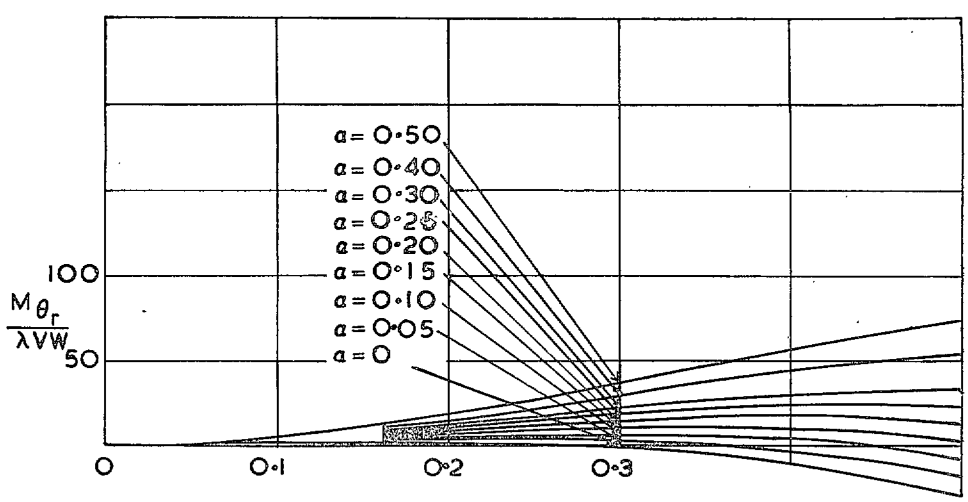

FIG. 20. Component of pitching moment ($M_{\theta T}/\lambda VW$) due to a positive angle of incidence at the stern (θ_T). Numerical example of Appendix III.

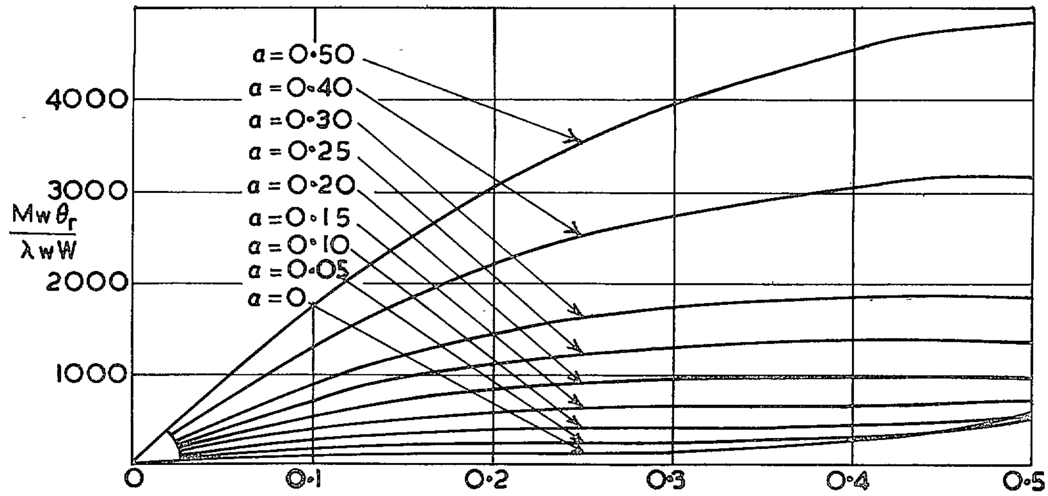

FIG. 21. Component of pitching moment ($M_\omega \theta_T/\lambda VW$) due to a positive angle of incidence at the stern (θ_T). Numerical example of Appendix III.

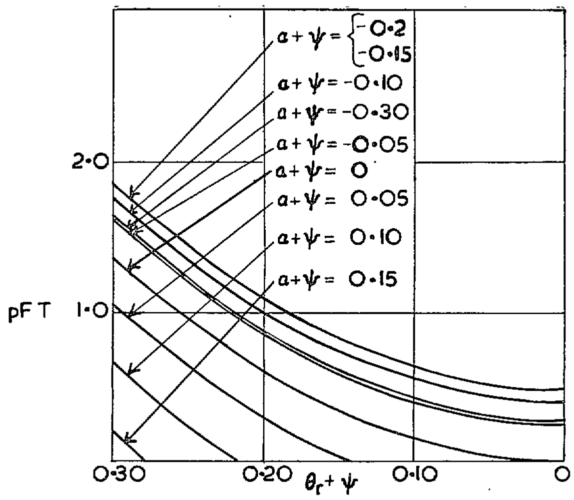

FIG. 22. Variation of penetration (p) with angles to horizontal of stern ($\theta_T + \psi$) and the central portion of keel ($\alpha + \psi$). Numerical example of Appendix III.

(692) Wt. 13/806 K.9 8/53 H.P.Co. 34-261

PRINTED IN GREAT BRITAIN

R. & M. No. 2574
(10,643)
A.R.C. Technical Report

Publications of the Aeronautical Research Council

ANNUAL TECHNICAL REPORTS OF THE AERONAUTICAL RESEARCH COUNCIL (BOUND VOLUMES)—

1936 Vol. I. Aerodynamics General, Performance, Airscrews, Flutter and Spinning. 40*s.* (40*s.* 9*d.*)
Vol. II. Stability and Control, Structures, Seaplanes, Engines, etc. 50*s.* (50*s.* 10*d.*)

1937 Vol. I. Aerodynamics General, Performance, Airscrews, Flutter and Spinning. 40*s.* (40*s.* 10*d.*)
Vol. II. Stability and Control, Structures, Seaplanes, Engines, etc. 60*s.* (61*s.*)

1938 Vol. I. Aerodynamics General, Performance, Airscrews. 50*s.* (51*s.*)
Vol. II. Stability and Control, Flutter, Structures, Seaplanes, Wind Tunnels, Materials. 30*s.* (30*s.* 9*d.*)

1939 Vol. I. Aerodynamics General, Performance, Airscrews, Engines. 50*s.* (50*s.* 11*d.*)
Vol. II. Stability and Control, Flutter and Vibration, Instruments, Structures, Seaplanes, etc. 63*s.* (64*s.* 2*d.*)

* 1940 Aero and Hydrodynamics, Aerofoils, Airscrews, Engines, Flutter, Icing, Stability and Control, Structures, and a miscellaneous section. 50*s.* (51*s.*)

* 1941 Aero and Hydrodynamics, Aerofoils, Airscrews, Engines, Flutter, Stability and Control, Structures. 63*s.* (64*s.* 2*d.*)

* 1942 Vol. I. Aero and Hydrodynamics, Aerofoils, Airscrews, Engines. 75*s.* (76*s.* 3*d.*)
Vol. II. Noise, Parachutes, Stability and Control, Structures, Vibration, Wind Tunnels. 47*s.* 6*d.* (48*s.* 5*d.*)

* 1943 Vol. I. (*In the press*).
Vol. II. (*In the press*).

* *Certain other reports proper to these volumes will subsequently be included in a separate volume.*

ANNUAL REPORTS OF THE AERONAUTICAL RESEARCH COUNCIL—

1933–34	1*s.* 6*d.* (1*s.* 8*d.*)	1937	2*s.* (2*s.* 2*d.*)
1934–35	1*s.* 6*d.* (1*s.* 8*d.*)	1938	1*s.* 6*d.* (1*s.* 8*d.*)
April, 1935 to Dec. 31, 1936.	4*s.* (4*s.* 4*d.*)	1939–48	3*s.* (3*s.* 2*d.*)

INDEX TO ALL REPORTS AND MEMORANDA PUBLISHED IN THE ANNUAL TECHNICAL REPORTS, AND SEPARATELY—

April, 1950 . . . . R. & M. No. 2600. 2*s.* 6*d.* (2*s.* 7½*d.*)

AUTHOR INDEX TO ALL REPORTS AND MEMORANDA OF THE AERONAUTICAL RESEARCH COUNCIL—

1909–1949 . . . . R. & M. No. 2570. 15*s.* (15*s.* 3*d.*)

INDEXES TO THE TECHNICAL REPORTS OF THE AERONAUTICAL RESEARCH COUNCIL—

December 1, 1936 — June 30, 1939.	R. & M. No. 1850.	1*s.* 3*d.* (1*s.* 4½*d.*)
July 1, 1939 — June 30, 1945.	R. & M. No. 1950.	1*s.* (1*s.* 1½*d.*)
July 1, 1945 — June 30, 1946.	R. & M. No. 2050.	1*s.* (1*s.* 1½*d.*)
July 1, 1946 — December 31, 1946.	R. & M. No. 2150.	1*s.* 3*d.* (1*s.* 4½*d.*)
January 1, 1947 — June 30, 1947.	R. & M. No. 2250.	1*s.* 3*d.* (1*s.* 4½*d.*)
July, 1951.	R. & M. No. 2350.	1*s.* 9*d.* (1*s.* 10½*d.*)

Prices in brackets include postage.

Obtainable from

HER MAJESTY'S STATIONERY OFFICE

York House, Kingsway, London, W.C.2; 423 Oxford Street, London, W.1. (Post Orders; P.O. Box 569, London, S.E.1); 13a Castle Street, Edinburgh 2; 39 King Street, Manchester 2; 2 Edmund Street, Birmingham 3; 1 St. Andrew's Crescent, Cardiff; Tower Lane, Bristol 1; 80 Chichester Street, Belfast OR THROUGH ANY BOOKSELLER.

S.O. Code No. 23-2574